BENG 207 Special Topics in Bioengineering

Neuromorphic Integrated Bioelectronics

Week 3: Silicon Cochlea

Gert Cauwenberghs

Department of Bioengineering
UC San Diego

http://isn.ucsd.edu/courses/beng207

BENG 207 Neuromorphic Integrated Bioelectronics

Date	Topic
9/27, 9/29	Biophysical foundations of natural intelligence in neural systems. Subthreshold MOS silicon models of membrane excitability. Silicon neurons. Hodgkin-Huxley and integrate-and-fire models of spiking neuronal dynamics. Action potentials as address events.
10/4, 10/6	Silicon retina. Low-noise, high-dynamic range photoreceptors. Focal-plane array signal processing. Spatial and temporal contrast sensitivity and adaptation. Dynamic vision sensors.
10/11, 10/13	Silicon cochlea. Low-noise acoustic sensing and automatic gain control. Continuous wavelet filter banks. Interaural time difference and level difference auditory localization. Blind source separation and independent component analysis.
10/18, 10/20	Silicon cortex. Neural and synaptic compute-in-memory arrays. Address-event decoders and arbiters, and integrate-and-fire array transceivers. Hierarchical address-event routing for locally dense, globally sparse long-range connectivity across vast spatial scales.
10/28, 11/1	Review. Modular and scalable design for neuromorphic and bioelectronic integrated circuits and systems. Design for full testability and controllability.
11/1, 11/3	Midterm due 11/2. Low-noise, low-power design. Fundamental limits of noise-energy efficiency, and metrics of performance. Biopotential and electrochemical recording and stimulation, lab-on-a-chip electrophysiology, and neural interface systems-on-chip.
11/8, 11/10	Learning and adaptation to compensate for external and internal variability over extended time scales. Background blind calibration of device mismatch. Correlated double sampling and chopping for offset drift and low-frequency noise cancellation.
11/15, 11/17	Energy conservation. Resonant inductive power delivery and data telemetry. Ultra-high efficiency neuromorphic computing. Resonant adiabatic energy-recovery charge-conserving synapse arrays.
11/22, 11/24	Guest lectures
11/29, 12/1	Project final presentations. All are welcome!

Mixed-Signal VLSI Robust Time-Frequency Feature Extraction

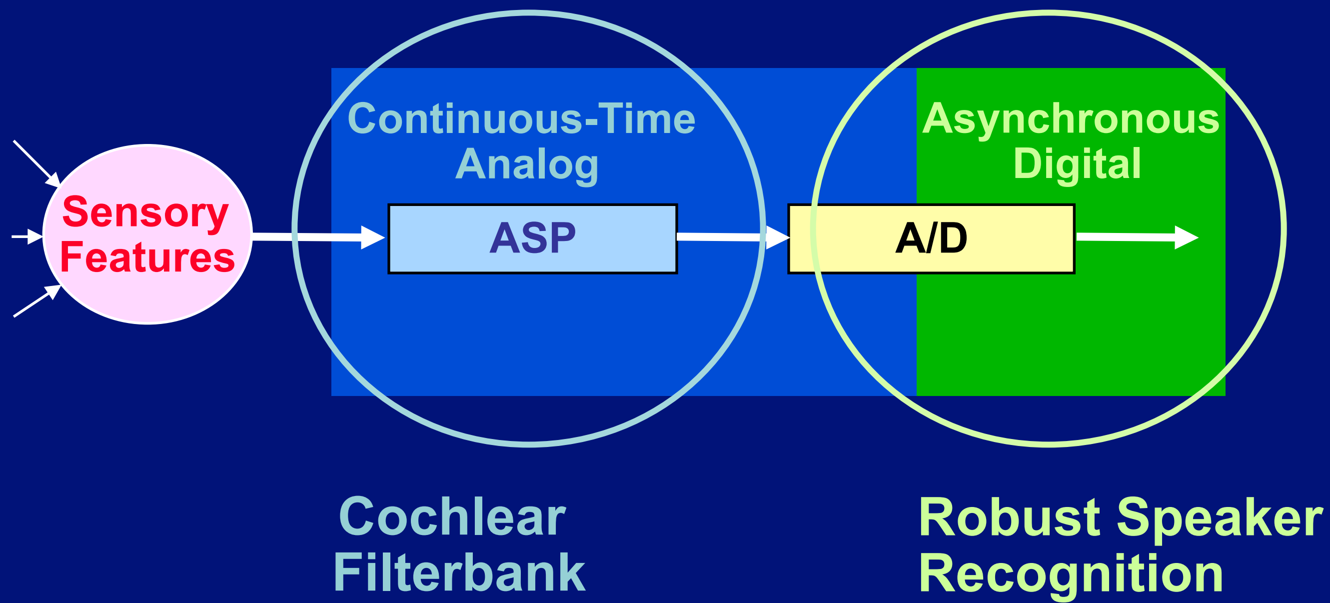

Pushing the Analog-Digital Boundary

- **Digital Sensory Processing:**

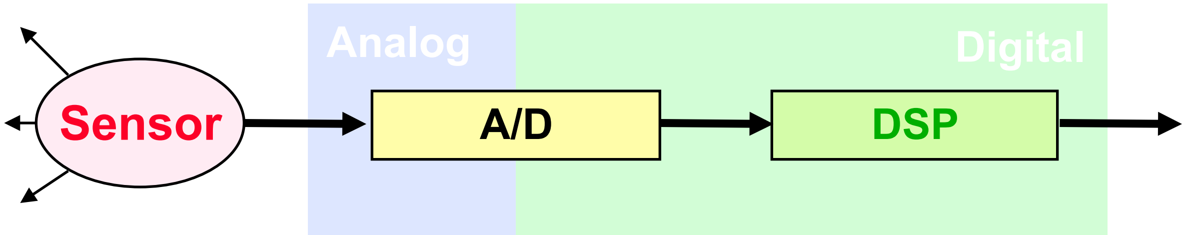

  - General-purpose
  - High precision (limited by A/D)

- **Analog and Mixed-Signal Sensory Processing:**

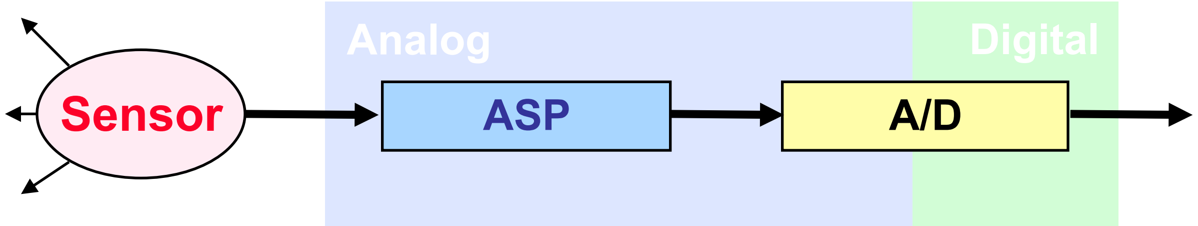

  - "Smart" A/D
  - Low power
  - Low complexity

Event-Driven Sensory Analog Processing

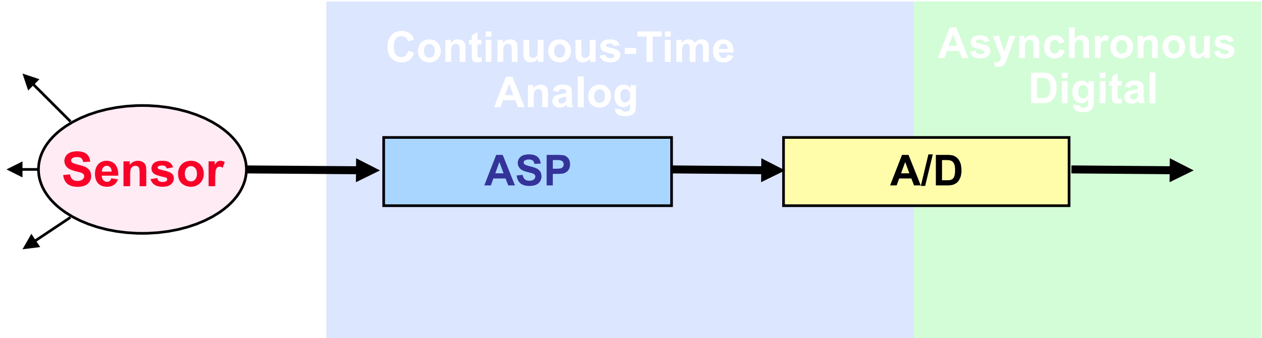

- **Data driven**
  - Communication bandwidth adjusts to information bandwidth in the signal
- **Asynchronous**
  - No quantization (binning) of time
  - No power-hungry clocks and synchronization across network nodes
- **Highly energy efficient**
  - Significant energy savings over Nyquist sampling for signals of sparse activity and medium amplitude resolution
- **Robust to additive noise in the signal**

Multi-Modal Event-Driven Sensory Analog Processing

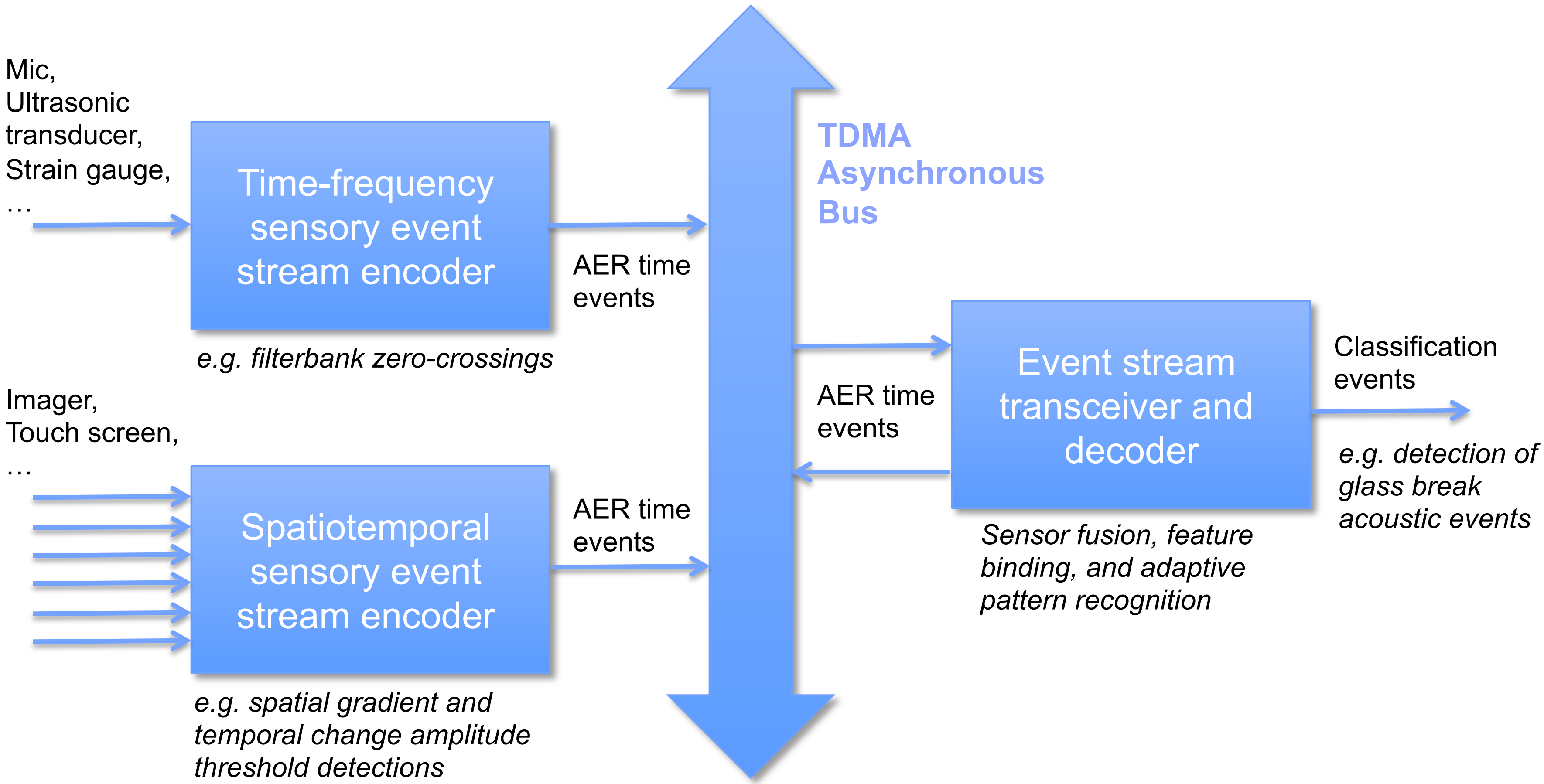

- Asynchronous routing of sensory address events
- Expandable dimensionality and integration of multiple sensory modalities
- Reconfigurable and adaptive general-purpose signal processing and identification

Auditory Anatomy and Modeling

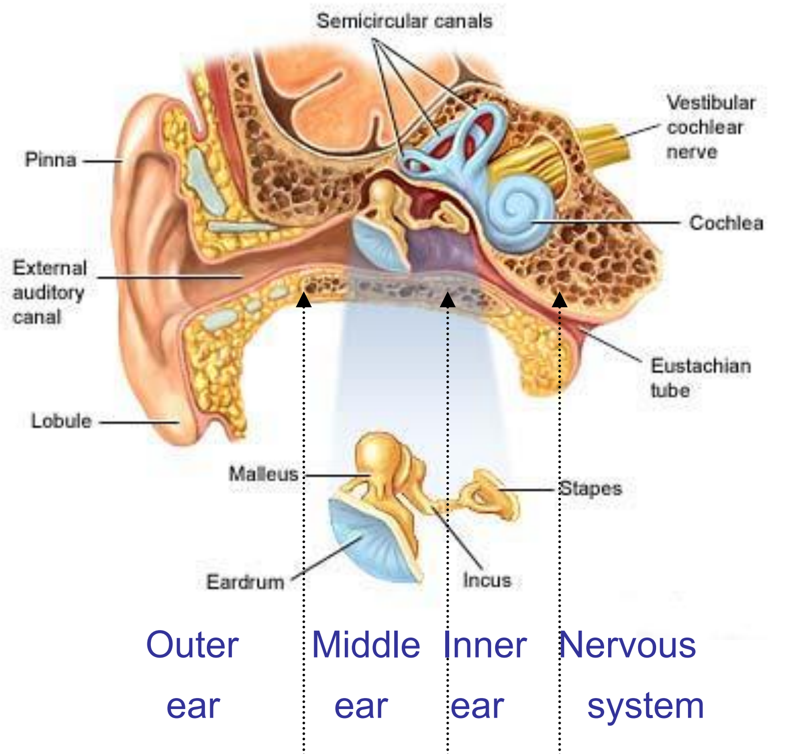

Ear Anatomy (adam.com)

Normal Hearing:

- **Outer ear** receives incoming acoustic wave
- **Middle ear** converts sound to mechanical vibration
- **Inner ear: cochlea** (a snail-shaped cavity filled with fluid), mechanical vibration -> fluid vibration -> displacement of **basilar membrane** (frequency information coding) -> bending of **hair cells**, releases neurochemicals -> firing of **auditory neuron** -> **central nervous system** (brain)

Abstraction for Speech Recognition:

- MFCC: Pre-emphasis, Mel-scale filter, Static nonlinear compression.
- Auditory perception model: + adaptive compression

Cochlea Cross Section

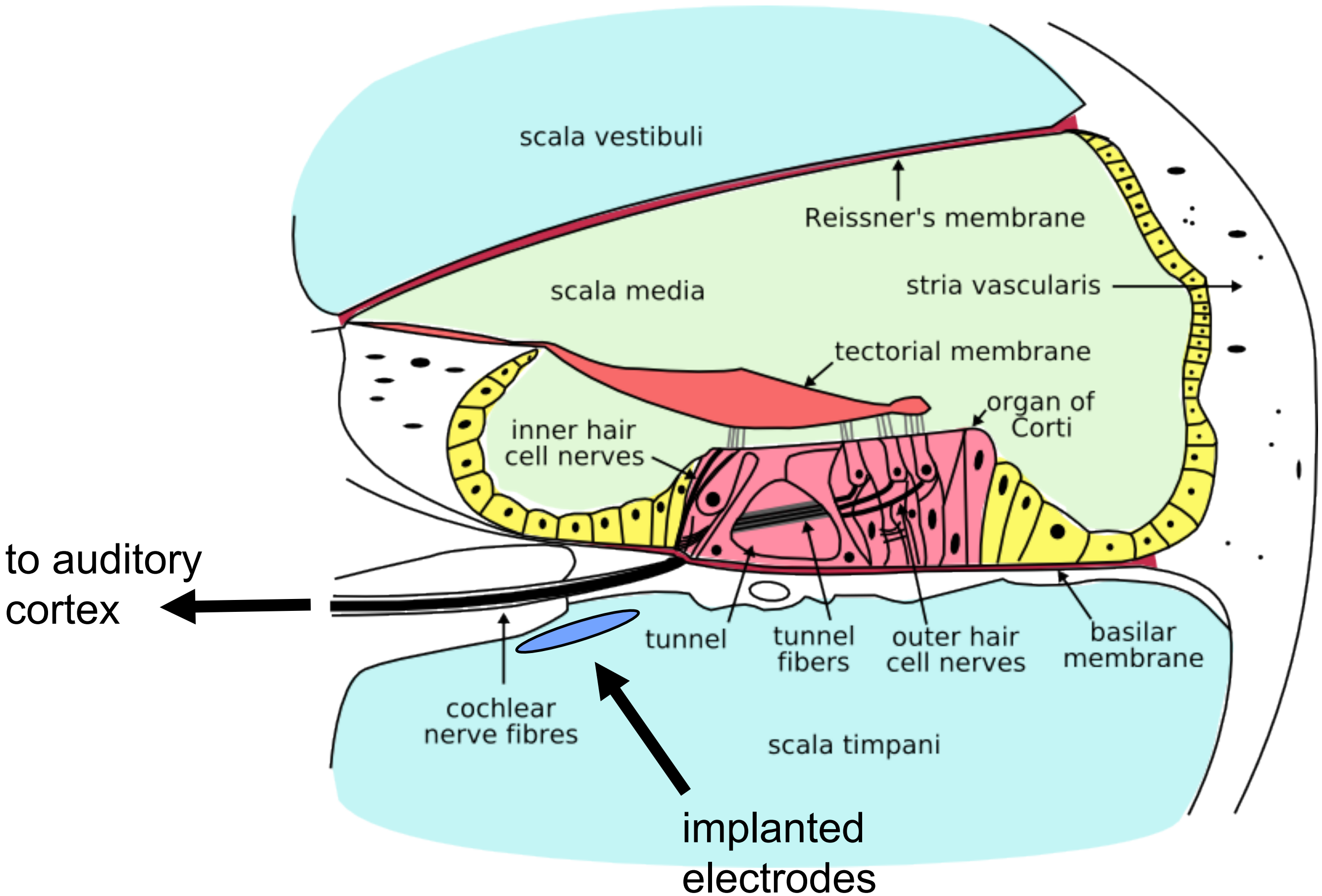

- Inner hair cells excited by basilar membrane vibrations, amplified by outer hair cells, stimulate cochlear nerve fibers in the healthy cochlea.
- Electrodes in the cochlear implant stimulate cochlear nerve fibers with alternating current signals, of amplitude representative of sound intensity.

http://en.wikipedia.org/wiki/Image:Cochlea-crosssection.png

Silicon Cochlea and Auditory Periphery

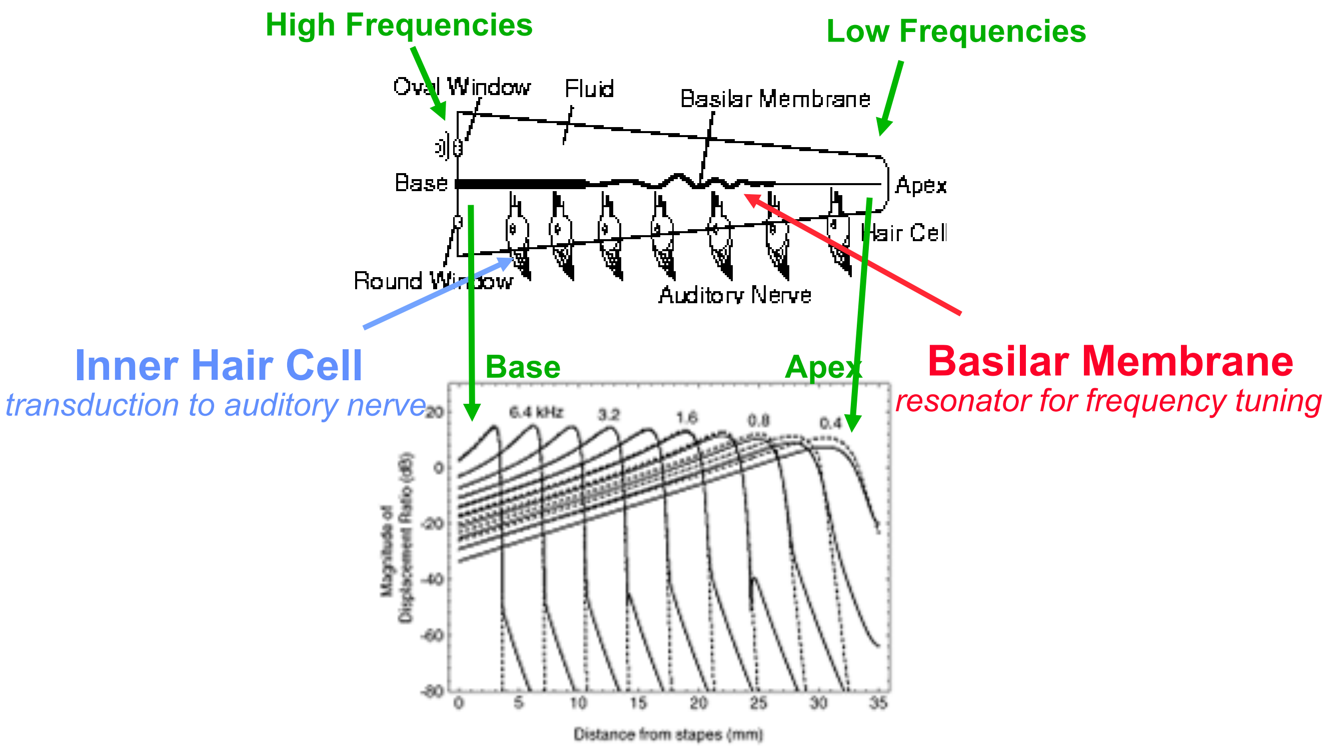

- Fluid-filled cochlea transduces sound to resonant mechanical vibrations of the basilar membrane
  - *Characteristic frequency-space coding*
- Hair cells transduce membrane deflections to auditory nerve impulses
  - *Amplitude and time encoding with spikes*

Silicon Cochlea and Auditory Periphery

Kumar, Cauwenberghs, and Andreou (1997)

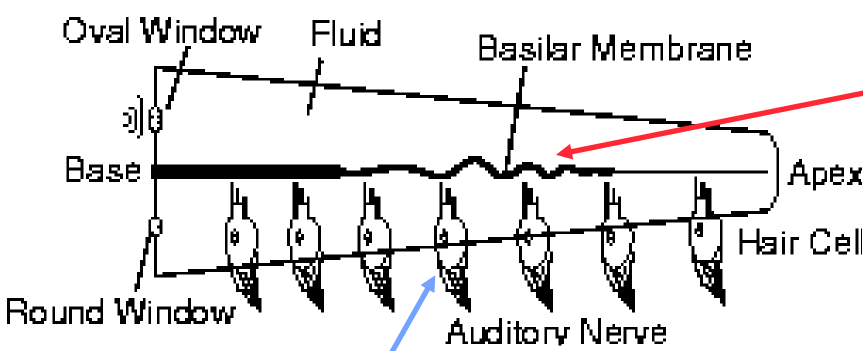

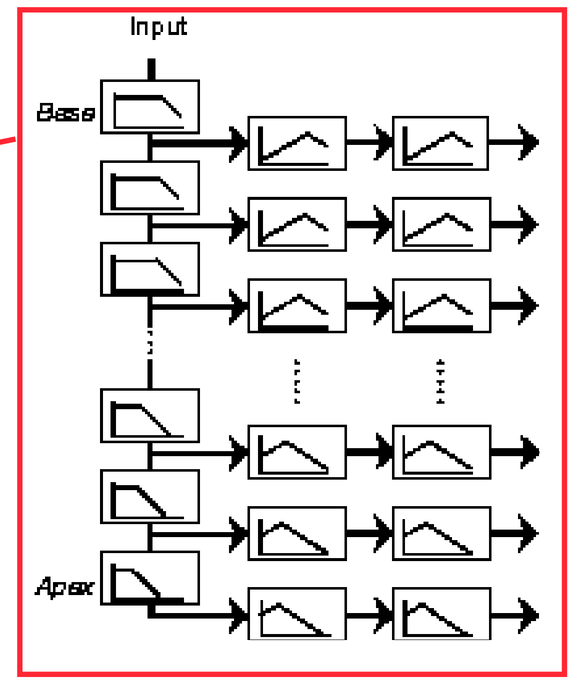

Basilar Membrane

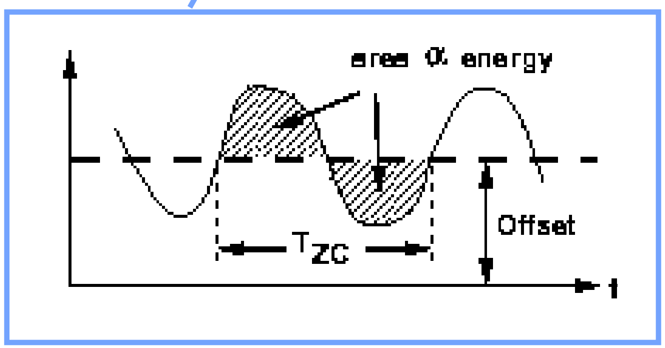

Hair Cell

Auditory Zero-Crossing Feature Extraction Chip

Kumar, Himmelbauer, Cauwenberghs, and Andreou (1998)

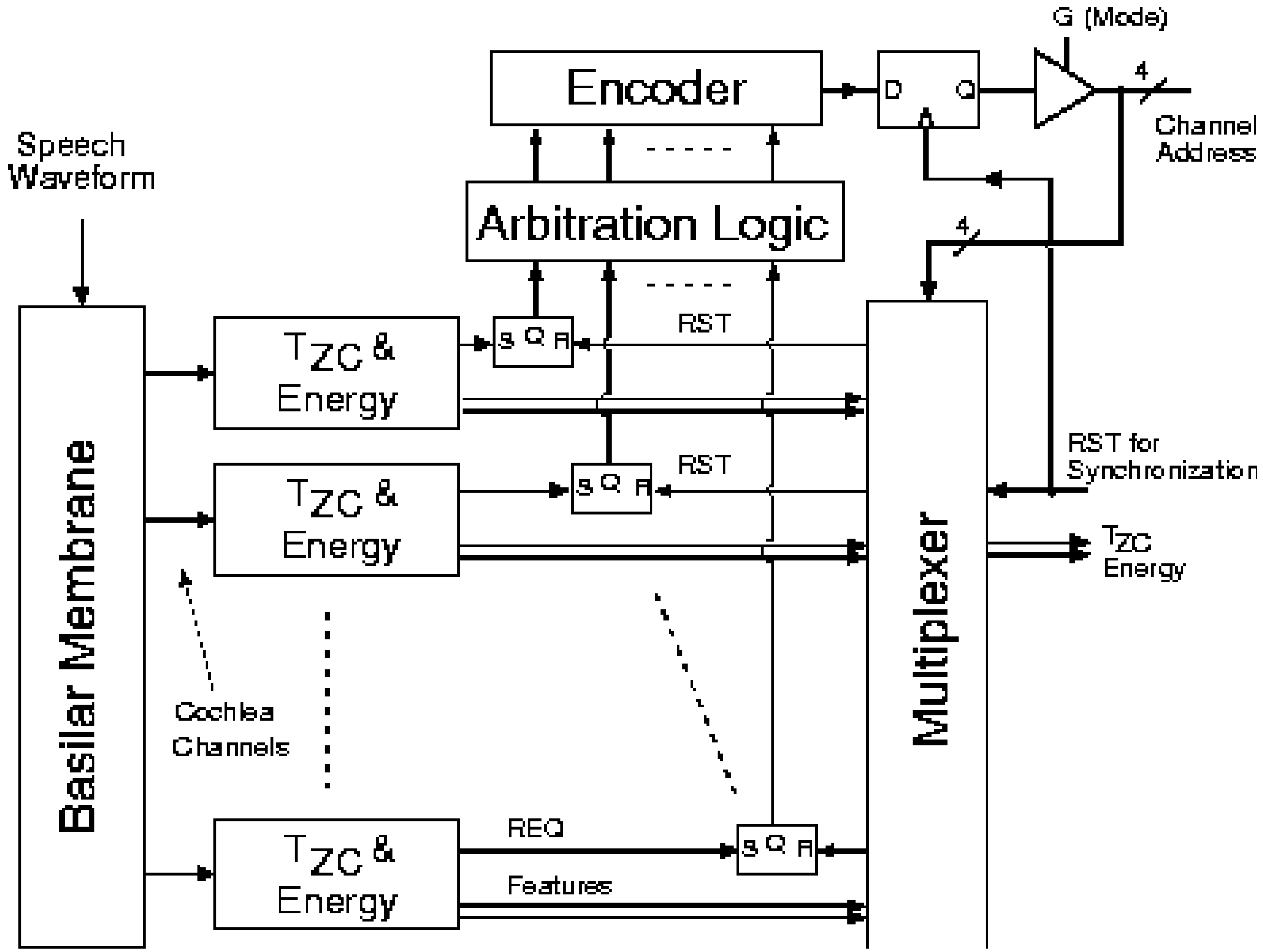

Auditory Zero-Crossing Feature Extraction Chip

Kumar, Himmelbauer, Cauwenberghs, and Andreou (1998)

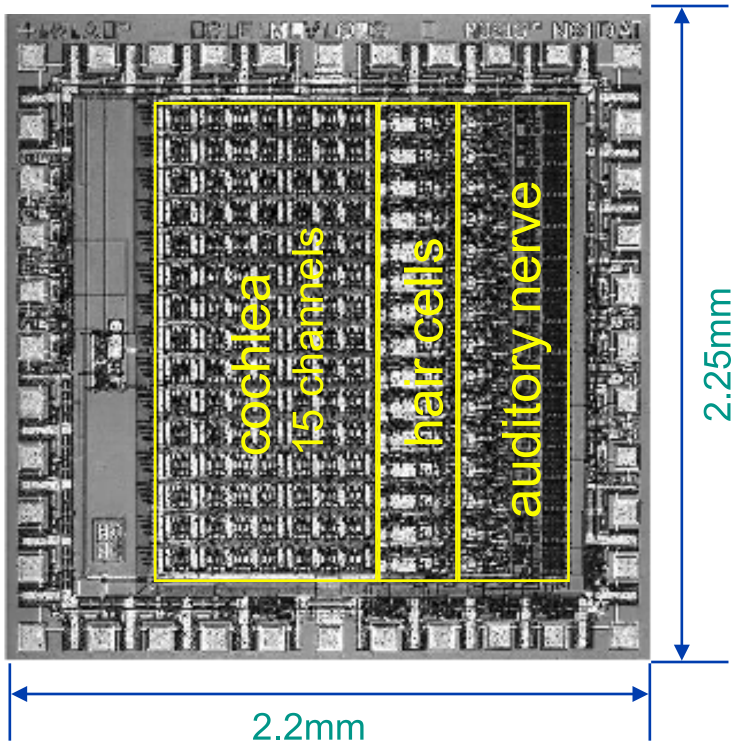

- 2mm X 2mm in 1.2μm CMOS
- 15 frequency channels
- asynchronous "spiking," address-event communication

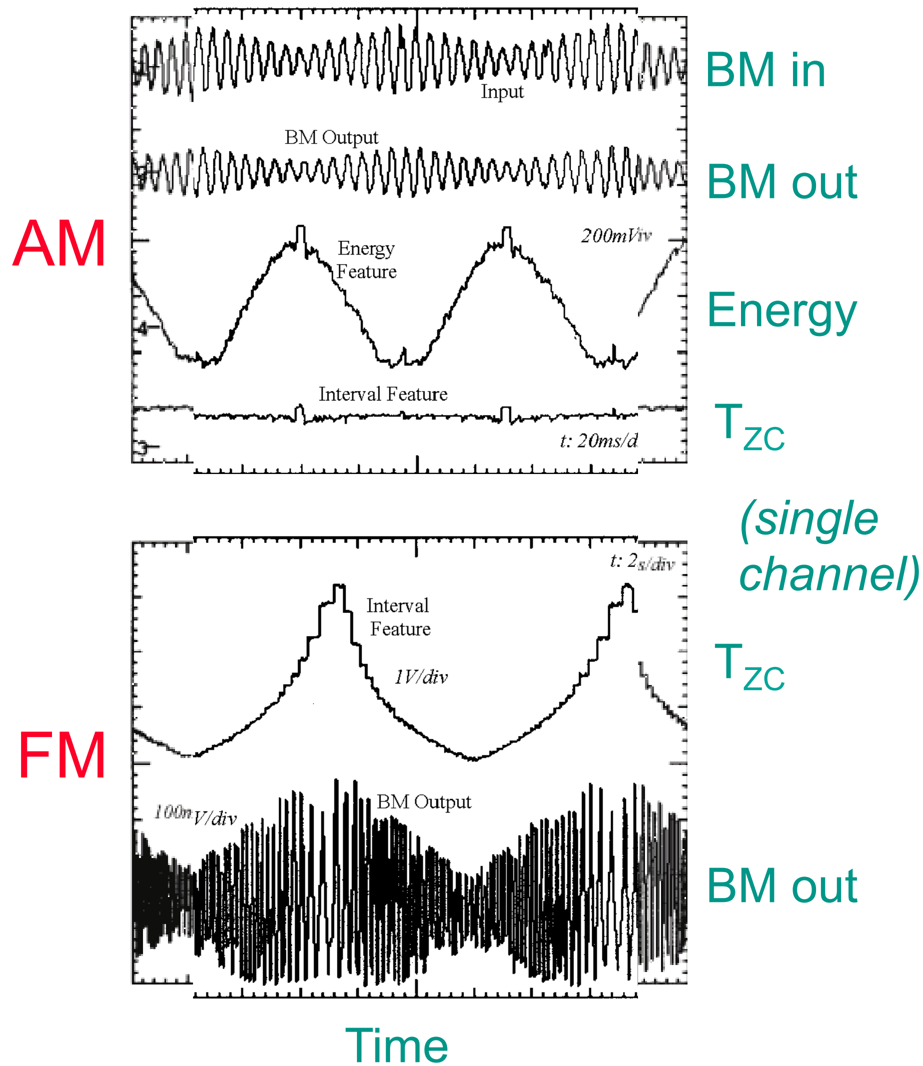

Auditory Zero-Crossing Feature Extraction Chip

Kumar, Himmelbauer, Cauwenberghs, and Andreou (1998)

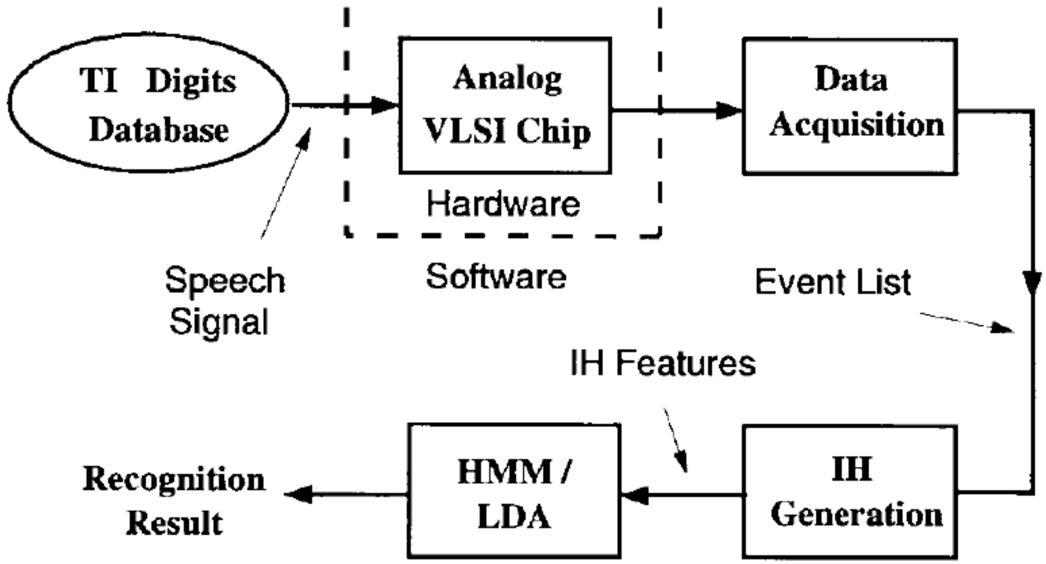

- Asynchronous ("spike") event features:
  - *Zero-crossing intervals*
  - *Energy*
- Linear discriminant analysis (LDA) transformed features are directly suitable for use with hidden Markov models (HMM) in speech recognition:
  - *99.47% recognition accuracy on TI-DIGITS*
  - *More robust to additive noise than mel-scale cepstral features*

Multi-Modal Event-Driven Sensory Analog Processing

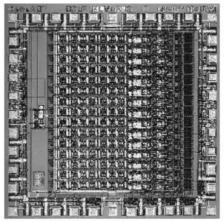

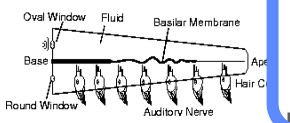

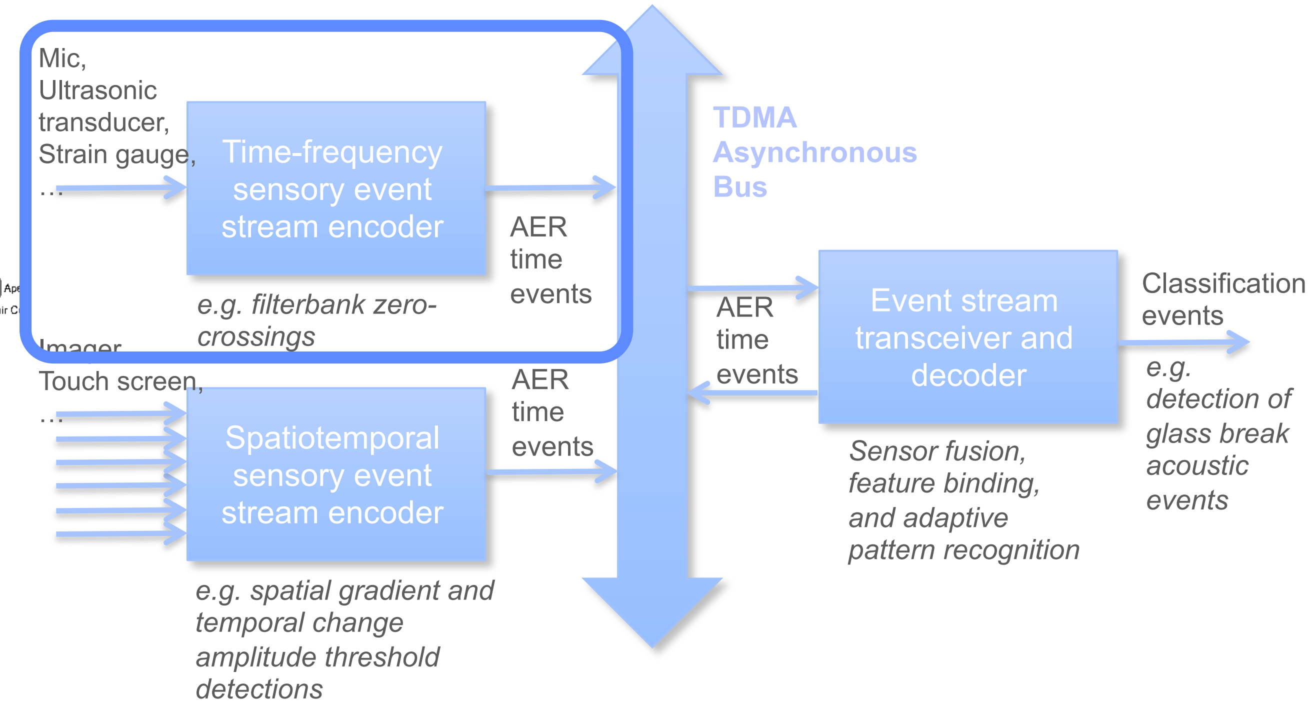

- **Time-frequency sensory event stream encoders:**
  - Convert a continuous-time analog sensory input, such as an acoustic signal, into an output stream of spike time events.
  - Time events correspond to time instances of zero-crossings of bandpass filtered versions of the signal.
  - Each bandpass filter with different center frequency is coded as a frequency address in the zero-crossing time event stream for distributed time-frequency encoding.

Integrated Pattern Recognition Adaptive Microsystems

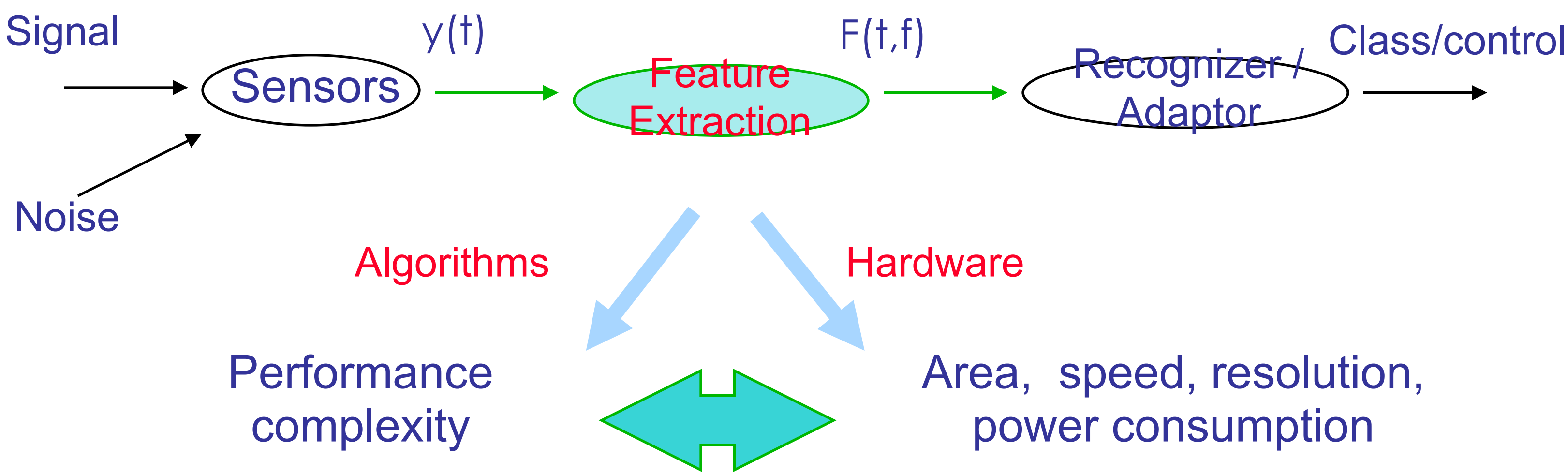

Ubiquitous sensing and computing:

Adaptive, Mobile, Sensory systems

Real-time, Low-power, Robust feature extraction

Parallel , Analog , Biomimetic computing

Time-Frequency Feature Extraction

Time-Frequency Analysis Methoc

- **Short-Time Fourier Transform (STFT)**
  Time-Frequency resolution limitation
- **Wavelet Transform**
  Multi-scale decomposition
  Better time frequency resolution
- **Filter Banks**
  Continuous time (no windowing)
  Multi-resolution (constant Q filter bank)

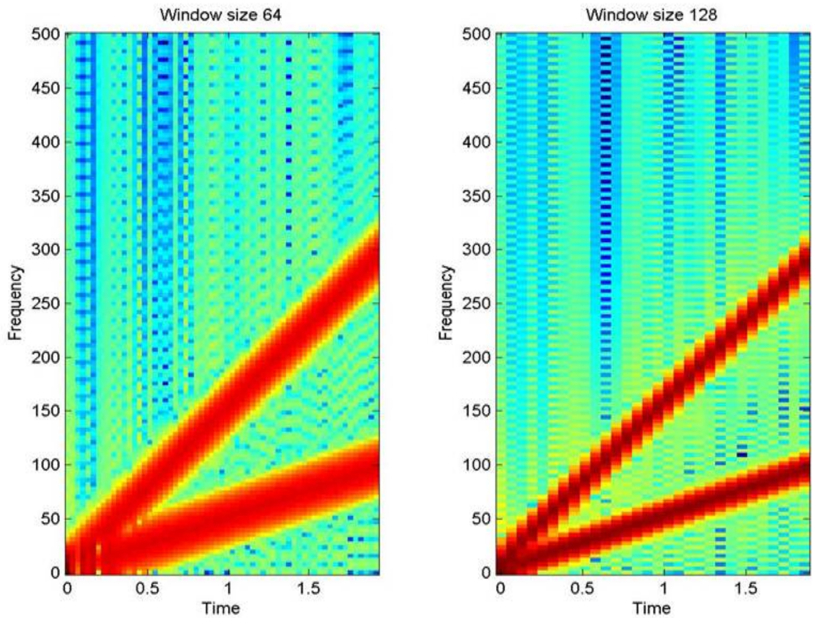

Which features to use?

- **Application dependent**
  speech / speaker / gender / emotion / language,/ …/ recognition,
- **Domain knowledge and methods combination**
  MFCC (Mel-frequency cepstral coefficients) features
  Combine auditory knowledge, SFTF, filter banks, ….
- **Feature selection**
  Maximize information content in feature extraction (Kumar' 96, Padmanabhan' 05)
  Experimental evaluation

Feature Extraction Chip Architecture

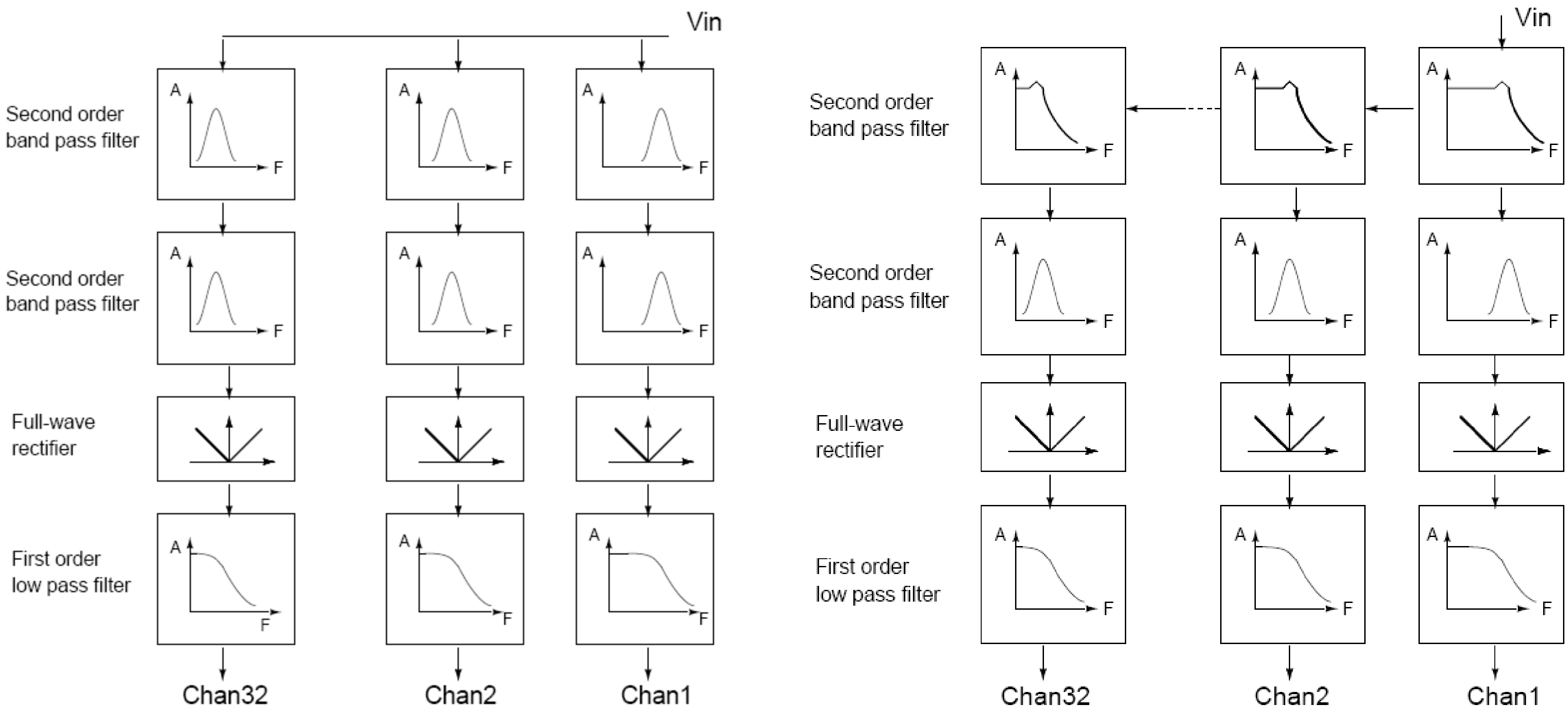

- Configurable parallel and cascade filter bank architecture
- 32 individually programmable channels:
  - Each channel: 2 biquad stages, full wave rectifier, and 1st order low-pass filter
    - biquad: programmable center frequency and Q-factor
    - low-pass filter: programmable cut-off frequency

Electronic Cochlea

Lyon and Mead (1988)

Operational transconductance amplifier (OTA)

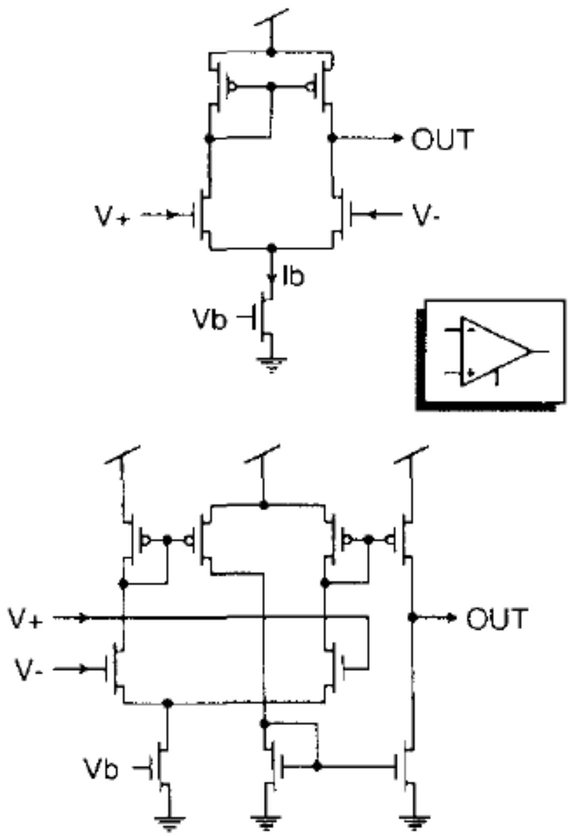

First-order section

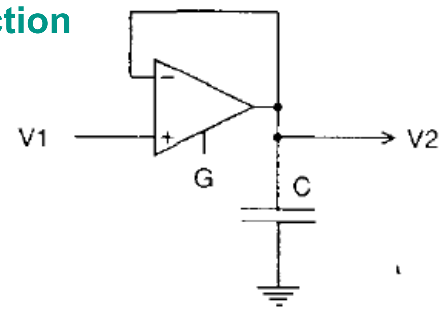

$$\frac{V_2}{V_1} = \frac{1}{\tau s + 1}$$

$$\tau = C/G$$

Second-order section

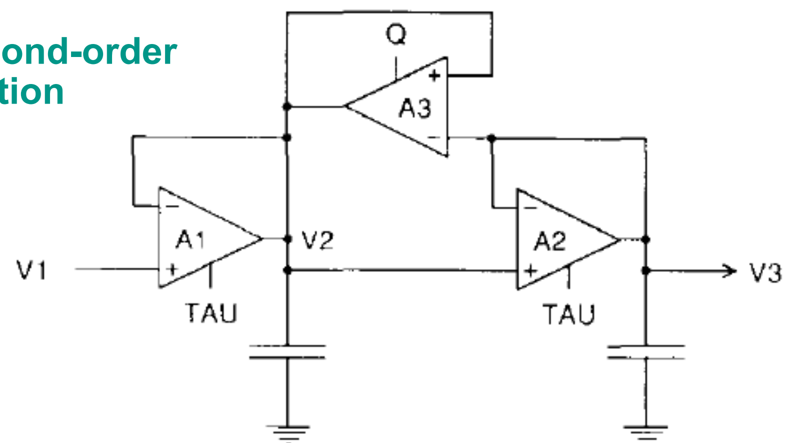

$$H(s) = \frac{V_3}{V_1} = \frac{1}{\tau^2 s^2 + 2\tau s(1 - \alpha) + 1}$$

$\tau = C/G$ and $\alpha = G_3/(G_1 + G_2)$.

R. Lyon and C.A. Mead, “Electronic Cochlea,” IEEE Trans. Acoustics, Speech, and Signal Processing (ASSP), 36 (7), 1988

Programmable Fully Differential OTA-C Filter

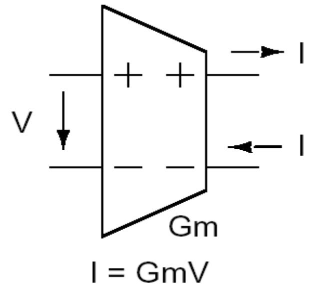

Fully differential OTA

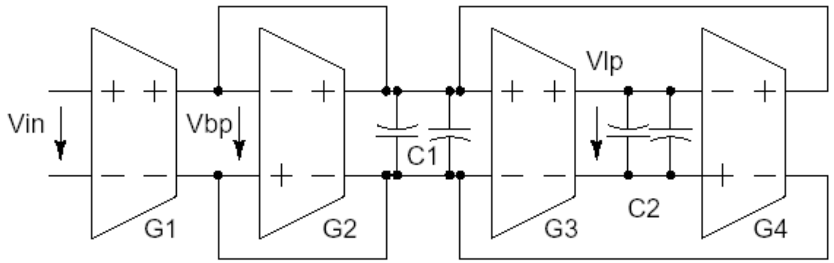

Second Order Band Pass and Low Pass Filter

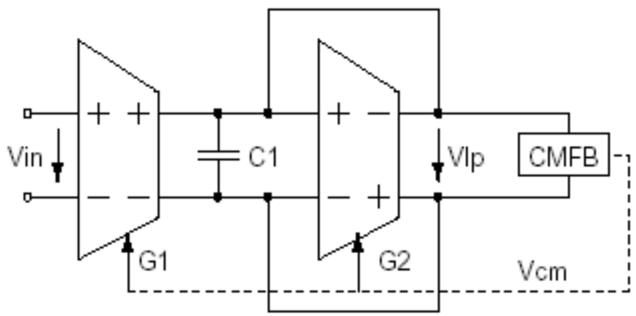

First Order Low Pass

$$H_{lp}(s) = \frac{\frac{G_1}{G_2}}{1 + s\frac{C_1}{G_2}}$$

$$H_{bp}(s) = \frac{s\frac{G_1}{C_1}}{s^2 + s\frac{G_2}{C_1} + \frac{G_3G_4}{C_1C2}} \qquad \omega = \sqrt{\frac{G_3G_4}{C_1C_2}}$$

$$H_{lp}(s) = \frac{\frac{G_1G_3}{C_1C_2}}{s^2 + s\frac{G_2}{C_1} + \frac{G_3G_4}{C_1C2}} \qquad Q = \sqrt{\frac{C_1G_3G_4}{C_2G_2^2}}$$

– Filter parameters (center frequency, quality factor, cut-off frequency) are a function of *Gm* and *C*
– Programmable *Gm* and selectable value of capacitance.

Three Decades Programmable OTA

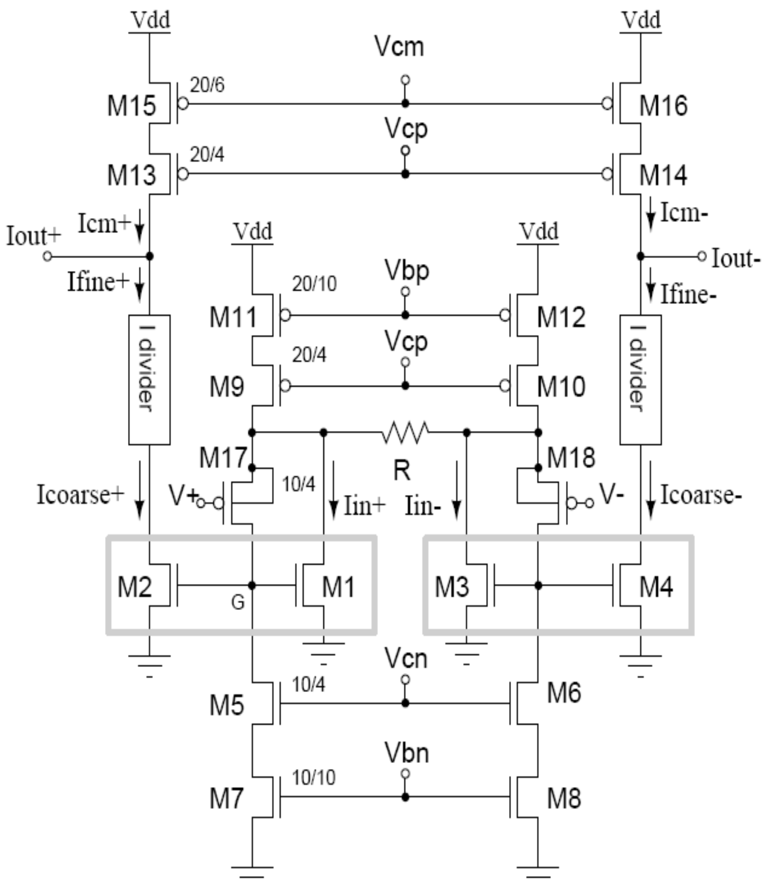

Fully differential configuration
- Doubled dynamic range, SNR
- Elimination of even order distortion
- High power supply rejection ratio (PSRR)
- Immunity to bias noise and variation

Differential pMOS input stage
- High input common mode rejection ratio
- Low 1/f noise

Integrated resistor source degeneration
- Wide input linear dynamic range

Multi-stage current scaling
- Multi-resolution, three decades *Gm* tuning

Cascode structure
- High output impedance

Current Scaling

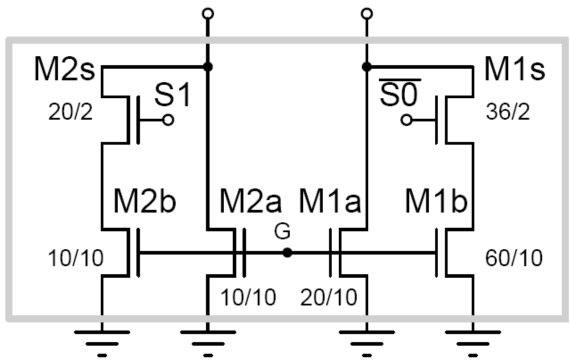

Coarse: 2-bit mirror with selectable W/L ratio
1:1, 1:2, 1:4, 1:8

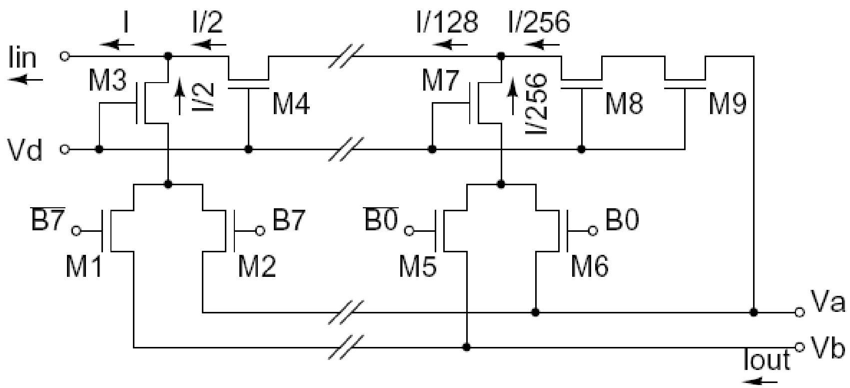

$$I_{out} = I_{in} \sum_{i=1}^{n} B_i 2^{-i}$$

Fine : 8-bit current divider

- Compact, four transistors per bit
- Wide current range
- Requires precise conveyer circuit to set Va and Vb at equal voltage

“**An Inherently Linear and Compact MOST-Only Current Division Technique**," K. Bult, Govert J. G. M. Geelen, *IEEE JSSC*, 1992.

Regulated Cascode Circuit

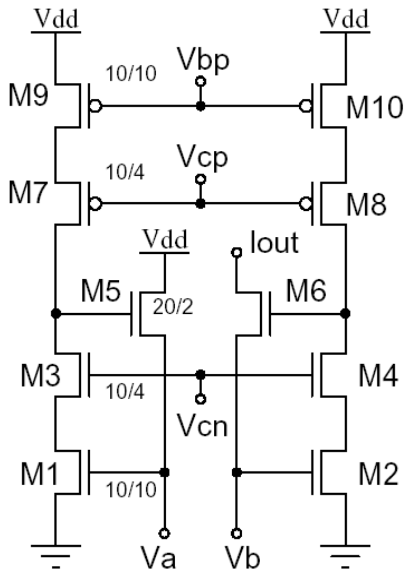

- Current conveyor
- Equates voltages Va and Vb
- Low input impedance

$$Z_{in} = \frac{1}{G_{m,6}(1 + G_{m,2}A_{cg,4}R_{out})}$$

- High output impedance

"A packaged low-noise high-speed regulated cascode transimpedance amplifier using 0.6 N-well CMOS technology" Sung Min Park and C. Toumazou, *ESSCC,* 2000.

Common Mode Feedback Circuit

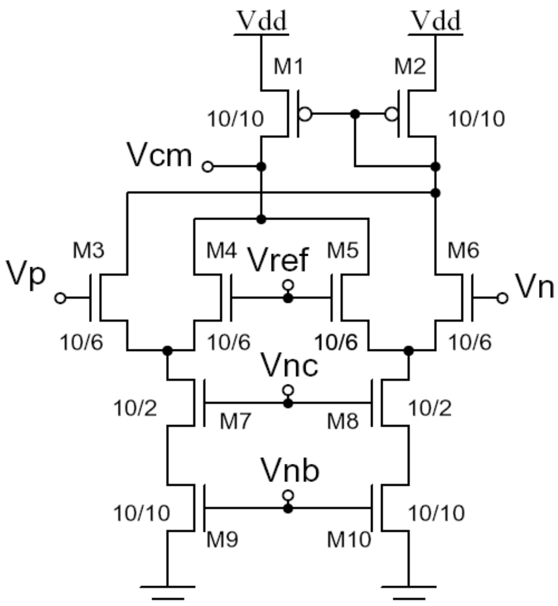

- High common mode gain
- Low differential mode gain
- *Vcm* sets common mode of *Vn* and *Vp* to *Vref*
- *Vref* is chosen to maximize linear dynamic range of OTA

"Design procedures for a fully differential folded-cascode CMOS operational amplifier"
Mallya, S. & Nevin, J.H.; JSSC, 1989

Silicon Implementation

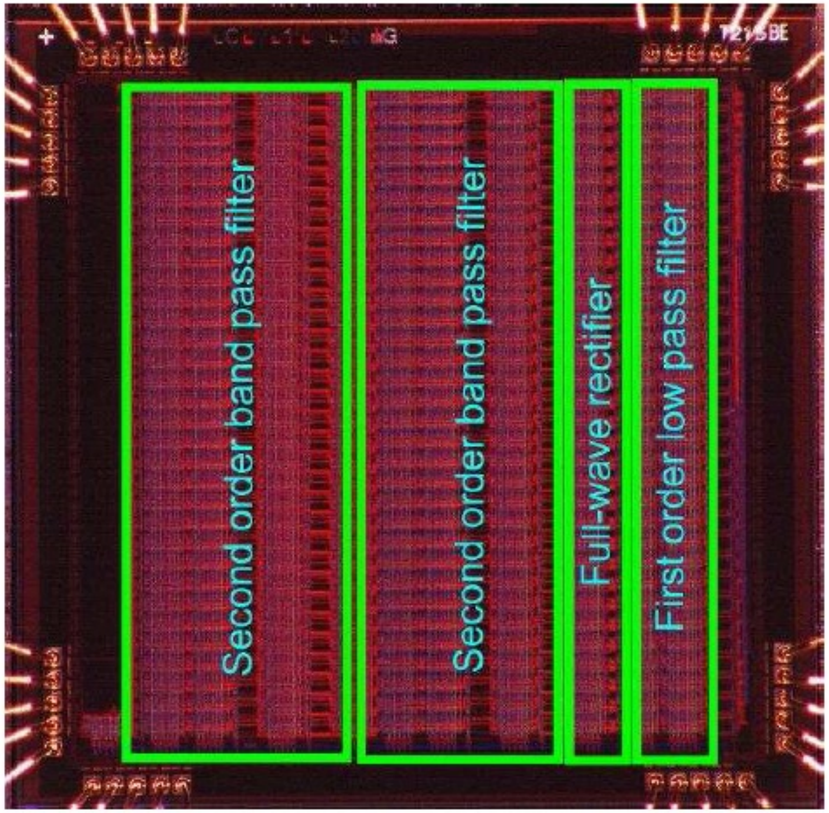

Photomicrograph of feature extraction chip

- **32-channel filter banks**
  - Parallel and cascaded configurable topologies
  - Total of 64 biquads and 32 first-order sections
- **Programmable filter parameter**
  - 320 OTAs with digitally programmable Gm
  - 180 capacitors with digitally selectable C
  - Cut-off/center frequency range: 100Hz-100Khz
  - Q range: 0.5-5
- **0.5um, 2P3M CMOS**
  - 3mm X 3mm
  - 9mW power

OTA Linear Range and Programmability

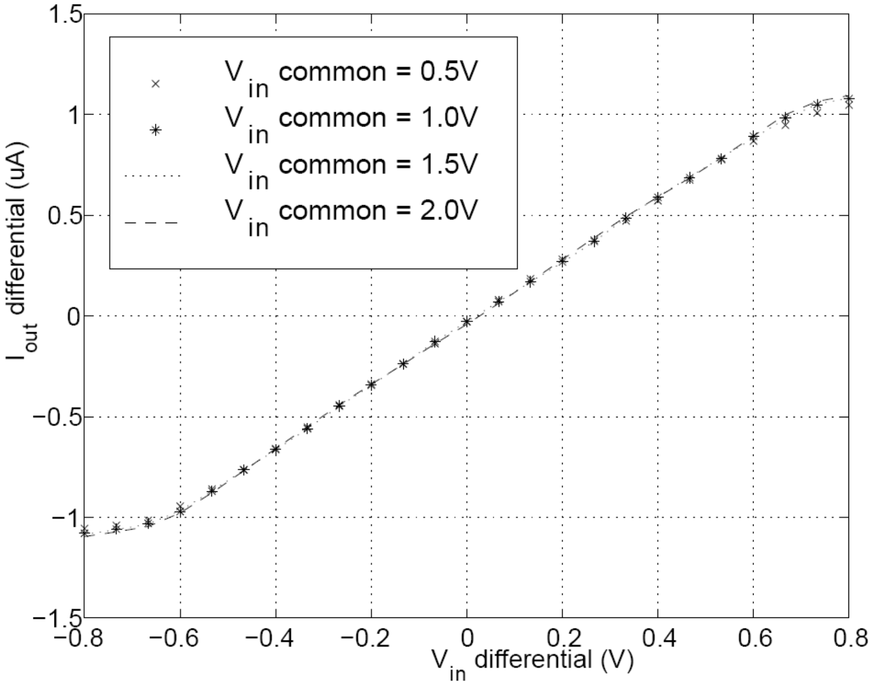

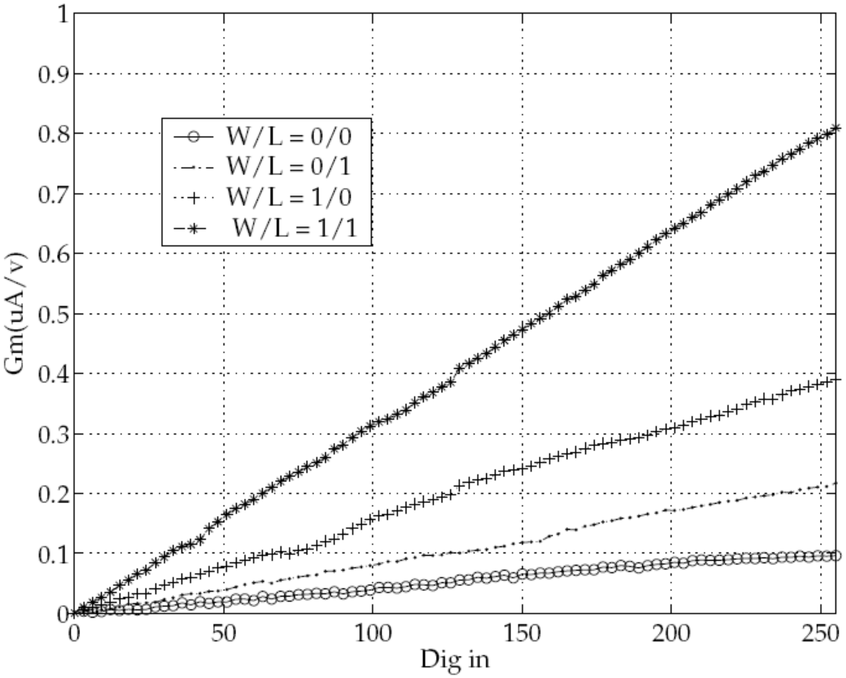

- Wide differential linear range, 2.4Vpp
- Wide common mode range, > 2V
- High common model rejection ratio, 40dB

- Multi-resolution programming,

  coarse 2 bits, fine 8 bits
- Wide programming range 1/2048

OTA Performance Summary

Parameter Specification	Measured
Max Gm	0.8 μA/V
Min Gm	0.39 nA/V
Programming ratio	1/2048
Input offset voltage	20 mV
Max dynamic input range	2.4 V_{pp}
Third order harmonic distoration	-48 dB @ 1V_{pp}
Common mode input voltage range	0.5-3 V
Common mode output voltage range	1.0-4.0 V
Common mode rejection ratio	40 dB
Power consumption	10 μW
Silicon area	0.014 mm^2
Power supply	5 V

"Three-Decade Programmable Fully Differential Linear OTA," Y. Deng, S. Chakrabartty and G. Cauwenberghs, *Proc. IEEE Int. Symp. Circuits and Systems (ISCAS'2004),* Vancouver Canada, 2004

Filter Parameter Sensitivity Analysis

$$
\begin{aligned}
f_o &= \frac{1}{2\pi}\sqrt{\frac{G_3 G_4}{C_1 C_2}} \\
Q &= \sqrt{\frac{C_1 G_3 G_4}{C_2 G_2^2}} \\
A_{bp} &= G_1/G_2
\end{aligned}
$$

$$
\delta f_o = \frac{f_o}{2}\left(\frac{\delta G_3}{G_3} + \frac{\delta G_4}{G_4} + \frac{\delta C_1}{C_1} + \frac{\delta C_2}{C_2}\right)
$$

$$
\begin{aligned}
\delta Q &= Q\left(\frac{\delta G_2}{G_2} + \frac{\delta G_3}{2G_3} + \frac{\delta G_4}{2G_4} + \frac{\delta C_1}{C_1} + \frac{\delta C_2}{C_2}\right) \\
\delta A_{bp} &= A_{bp}\left(\frac{\delta G_1}{G_1} + \frac{\delta G_2}{G_2}\right).
\end{aligned}
$$

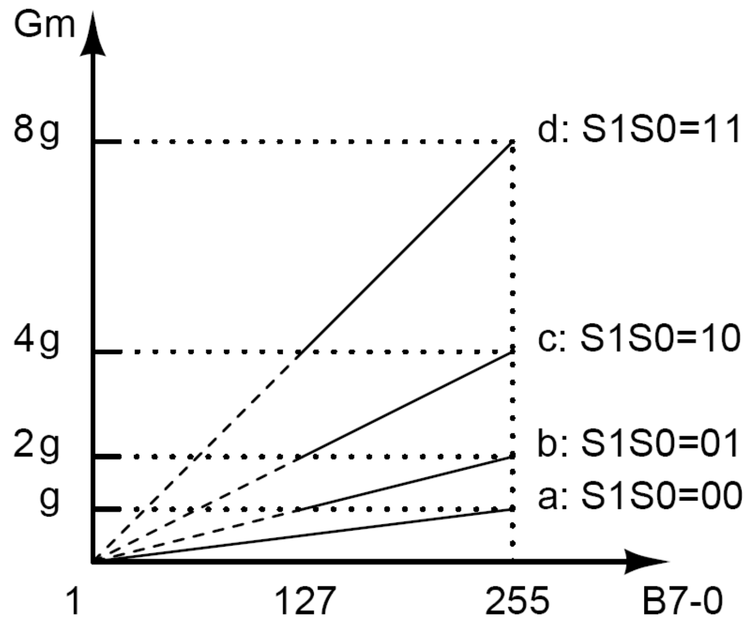

Multi-resolution programming, to minimize sensitivity of center frequency.

Define $G^* = 2\pi f_o \sqrt{C_1 C_2}$

If $G^* \in (0, g] \cup (\sqrt{2}g, 2g)] \cup (2\sqrt{2}g, 4g)] \cup (4\sqrt{2}g, 8g]$ choose $G_3 = G_4 = G^*$

Otherwise, $G_3 = G^*/\sqrt{2}, G_4 = \sqrt{2}G^*$

Filter Parameter Non-idealities

Non-idealities of OTA: offset, limited linear range, finite output impedance, finite common mode rejection, …

$$f_o = \frac{1}{2\pi}\sqrt{\frac{G_3G_4}{C_1C_2}}$$
$$Q = \sqrt{\frac{C_1G_3G_4}{C_2G_2^2}}$$
$$A_{bp} = G_1/G_2$$

Ideal, independently programmable

$\xrightarrow{}$ Finite OTA output impedance

$$f_o = \frac{1}{2\pi}\sqrt{\frac{G_3G_4 + G_2/R_o + 3/(R_o^2)}{C_1C_2}}$$
$$Q = \sqrt{\frac{C_1(G_3G_4 + G_2/R_o + 3/R_o^2)}{C_2(G_2 + (C_1/C_2 + 3)/R_o)^2}}$$
$$A_{bp} = \frac{G_1}{G_2 + (C_1/C_2 + 3)/R_o}.$$

Implemented

Filter parameters are no longer independently programmable

- OTA nonlinear macro model (Gomez’ 95)
- Response surface method for continuous time filter (Malik’ 05)

Generalized linear model for filter parameter modeling and calibration

Filter Parameter Modeling and Calibration

•**Generalize Linear Model:**

$$\begin{aligned}
log f_o &= a_0 + a_1 logG_1 + a_2 logG_2 + a_3 logG_3 + a_4 (logG_1)^2 + \\
&\quad a_5 logG_1 logG_2 + a_6 logG_1 logG_3 + a_7 (logG_2)^2 + \\
&\quad a_8 logG_2 logG_3 + a_9 (logG_3)^2 + a_{10} (logG_1)^3 + \ldots \\
logQ &= b_0 + b_1 logG_1 + b_2 logG_2 + b_3 logG_3 + b_4 (logG_1)^2 + \ldots \\
log A_{bp} &= c_0 + c_1 logG_1 + c_2 logG_2 + c_3 logG_3 + c_4 (logG_1)^2 + \ldots
\end{aligned}$$

Modeling procedure:

1. Data sample schema: choose modeling region of interest, given target characteristic determine least sensitivity values for programming bits.
2. Sample data: program filter, sweep frequency, measure filter parameters.
3. Build Model: determine *a*(*i*), *b*(*i*), *c*(*i*) by least squares error linear regression.

Calibration:

$$\arg\min_{logG_i} \{W_f (log f_o - \log(T_F))^2 + W_Q (logQ - \log(T_Q))^2 + W_A (logA - \log(A))^2\}$$

$$\log(2^{S_0 S_1}) \leq logG_i \leq \log(255 * 2^{S_0 S_1})$$

Gm-C Filter Response

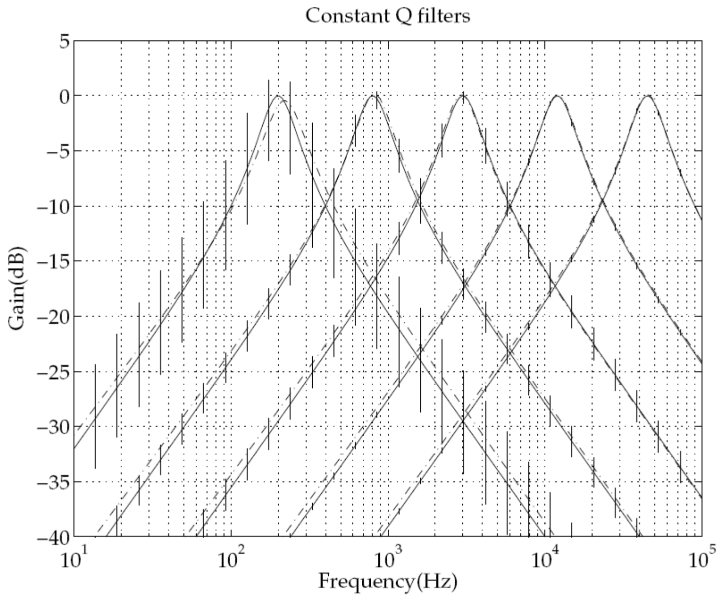

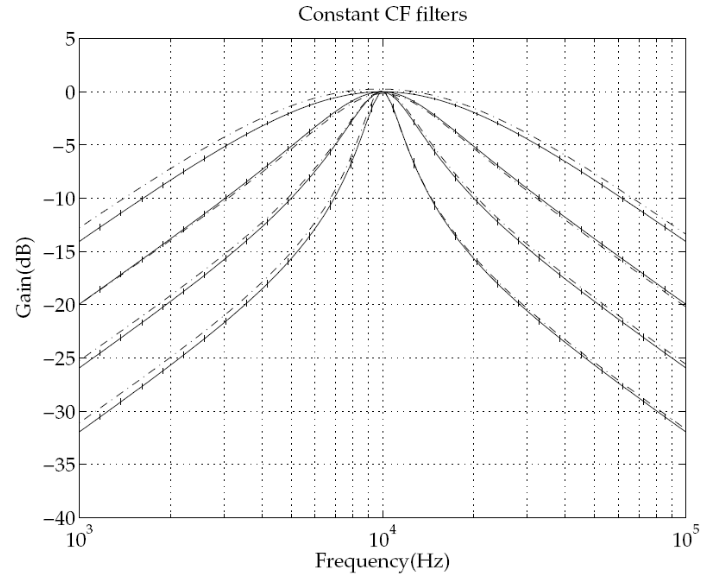

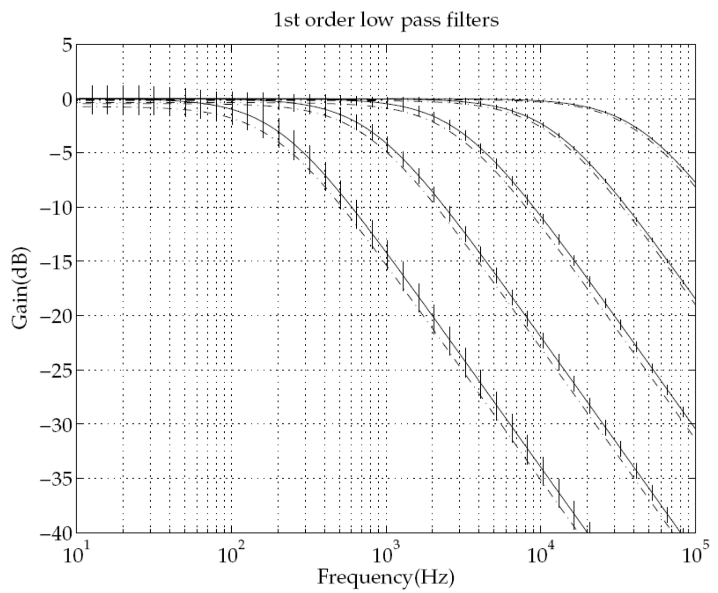

Measured and predicted response

- programmable center frequency, Q, gain, and cut-off frequency.
- programming range:
  CF: 100Hz-100 kHz;
  Q: 0.5-5.

Biquad Performance Summary

Parameter Specification	Measured
Filter type	second order bandpass and low-pass
Center Frequency	100 KHz
Silicon area	0.06 mm^2
Power consumption	100 μW (@1Vpp input)
Input referred noise	865μV
Differential input range	2V_{pp} (@THD=-42dB)
Dynamic range	61 dB (@THD=-42dB)
Stop-band rejection	32 dB (for low-pass)
Passband ripple	0.24 dB (for low-pass)
CMRR	40 dB
PSRR	39 dB

Application: Robust Speech Recognition

Speech segment with various samples of additive noise from NOISEX-92 database, at 10dB SNR.

- Clean

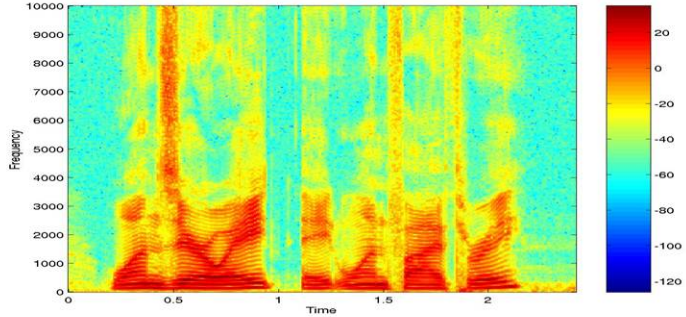

- Factory

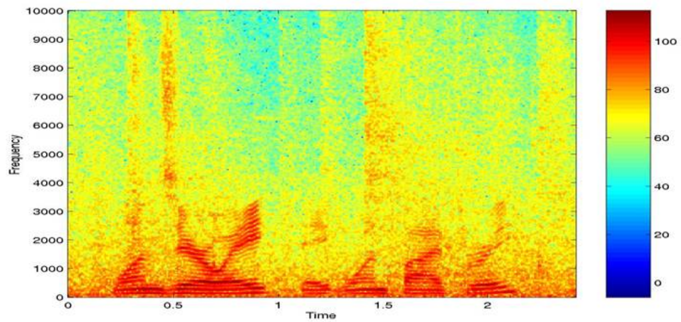

- White

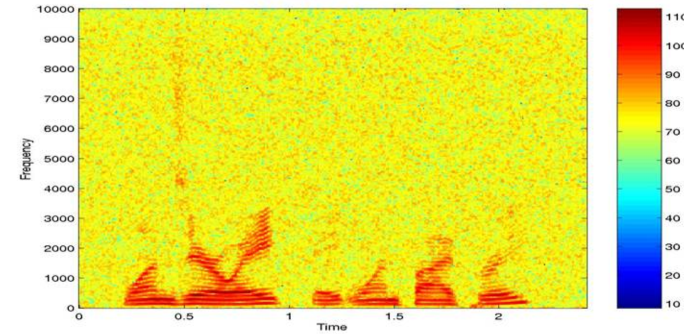

- Car

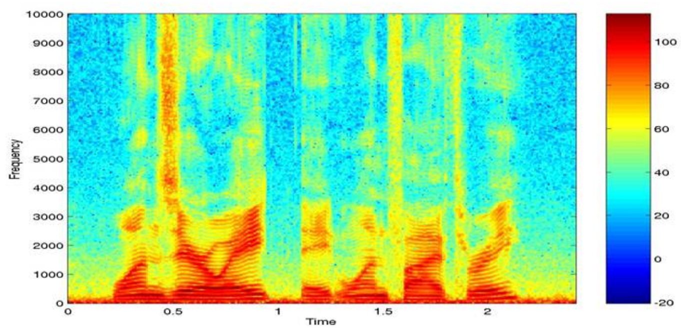

Babble

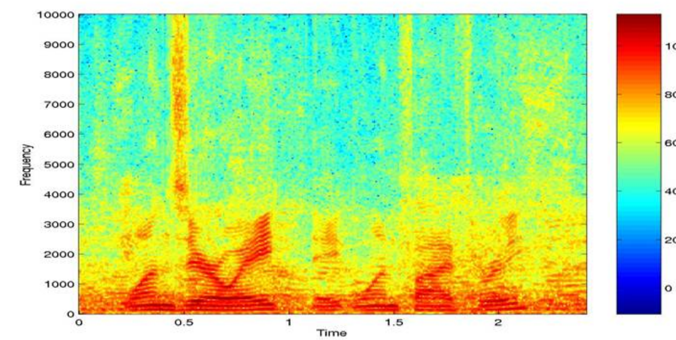

Auditory Perception Model

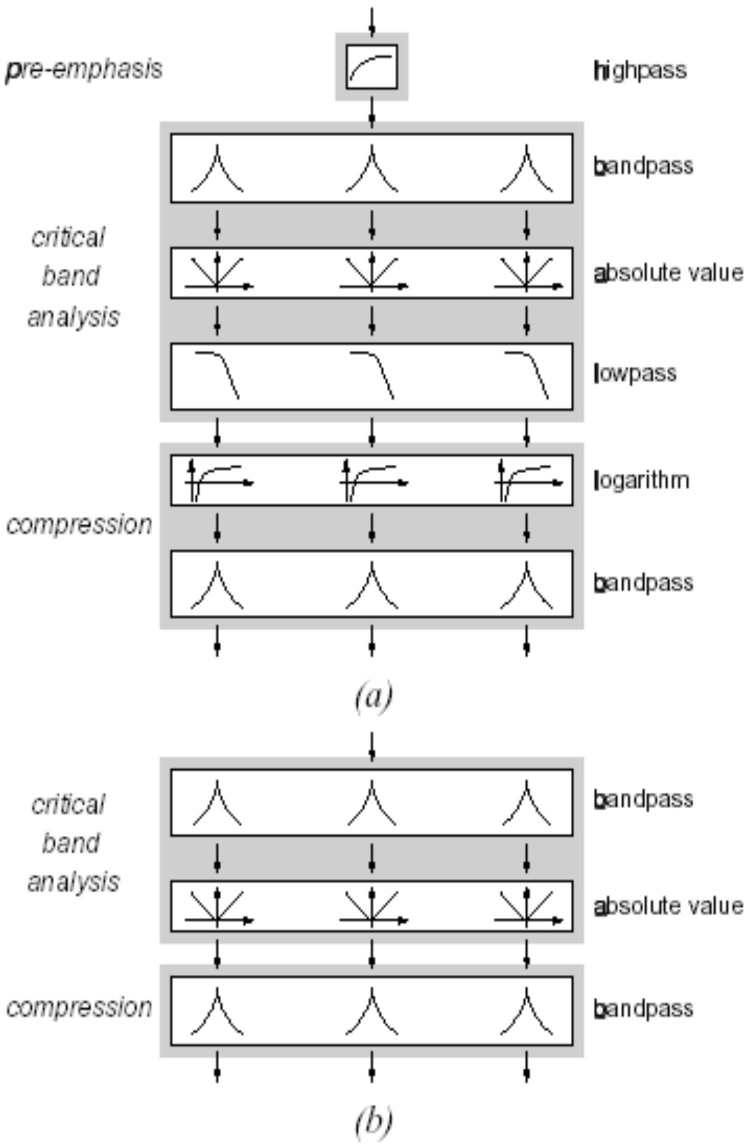

- **Pre-emphasis:** middle ear, 50Hz highpass cut-off
- **1st Band-pass:** basilar membrane; frequency tuned place coding
- **Full-wave rectifier:** hair cell; extracts magnitude envelope information
- **Log:** static non-linear compression
- **2nd Band-pass:** adaptive non-linear compression (Tchorz 99).

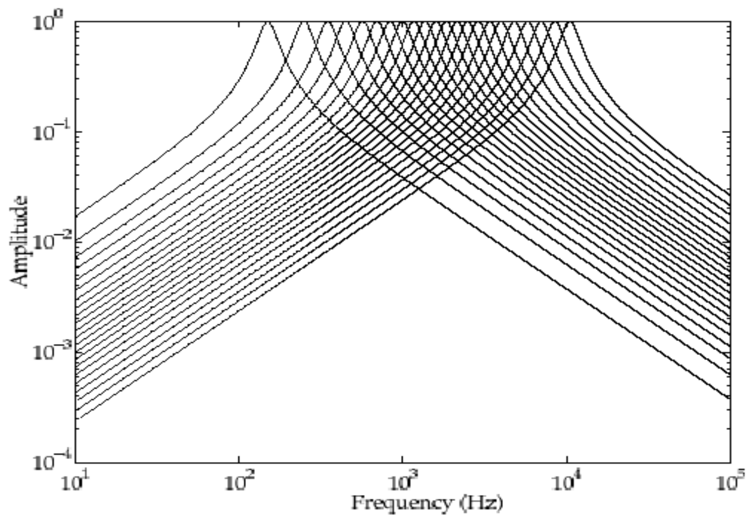

$$H_i(s) = \frac{G\frac{\omega_i}{Q}s}{s^2 + \frac{\omega_i}{Q}s + \omega_i^2} \qquad i = 1, \ldots 24$$

MFCC vs. Auditory Features on Isolated TI-Digit Database

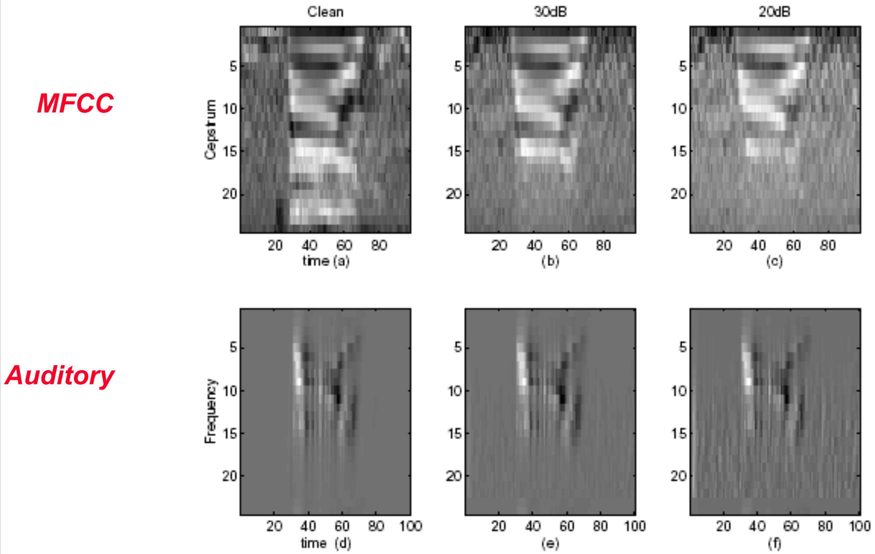

Experiment conditions:

- 14 states left to right hidden Markov model (HMM) for each digit
- 12 dimension feature by discrete cosine transform (DCT)
- 4 mixture Gaussian model
- 770 clean training utterances
- Tested on 440 utterances added with noise of different statistics
- Hidden Markov model toolkit (HTK)

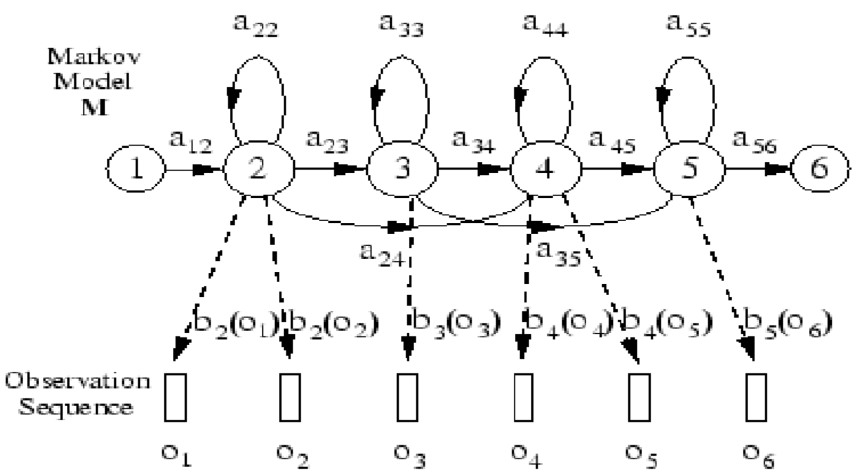

The Markov Generation Model

Training:

Maximum likelihood parameter estimation through Expectation Maximization (EM) algorithm

Testing:

$\arg\max_W \{P(W|O)\}$, Bayes rule

Experimental Results

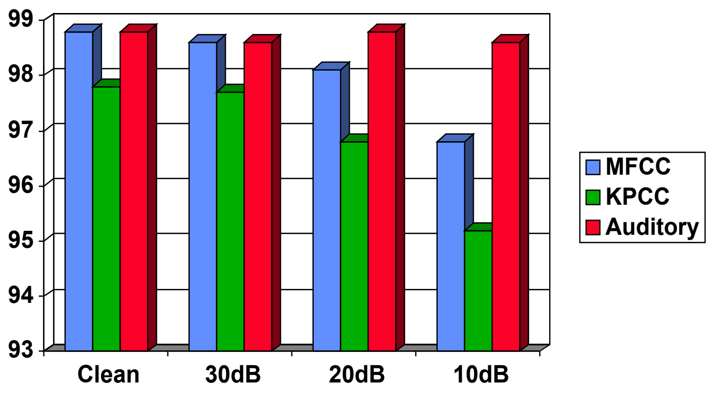

Car noise

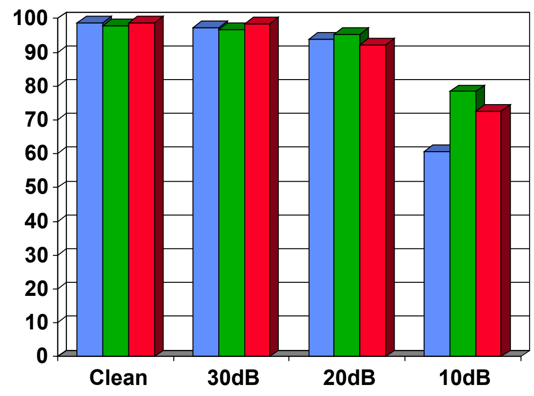

Babble noise

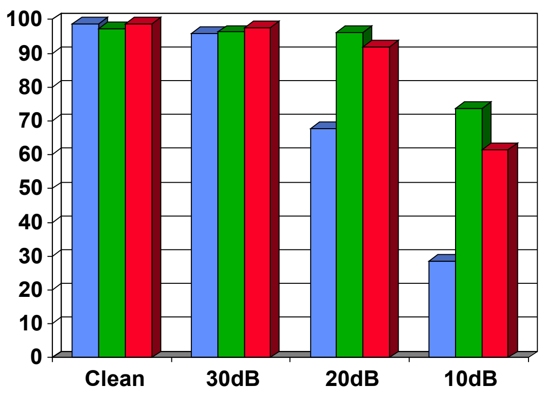

Factory noise

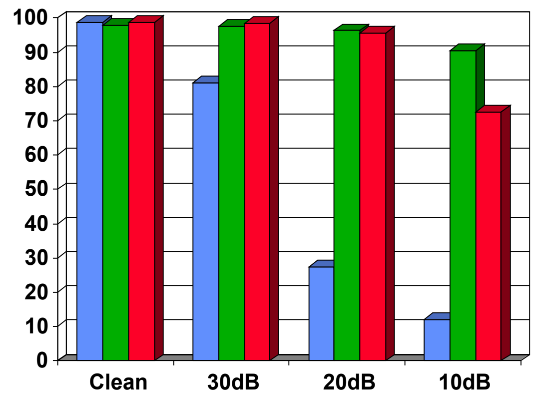

White noise

"**Analog Auditory Perception Model for Robust Speech Recognition**," Y. Deng, S. Chakrabartty and G. Cauwenberghs, *IEEE Int. Joint Conf. Neural Networks*, 2004.
"**Robust Speech Feature Extraction by Growth Transformation in Reproducing Kernel Hilbert Space**," S. Chakrabartty, Y. Deng and G. Cauwenberghs, Proc. IEEE, ICASSP'2004.

YOHO Text-independent Speaker Recognition

'Yoho' speech identification database

- 6 continuous digits per utterance
- 10 male speakers are chosen
- 30 clean utterances per speaker for enrollment
- 20 utterances per speaker for identification

Speech Feature

- Clean speech, and speech with additive noise of various statistics
- 12 dimensional feature vectors, MFCC vs. auditory model (Q1=7)
- Different from features used for speech recognition (Q1=4)

Training and Testing

- Trained on clean speech, tested on clean and noisy speech
- Gaussian mixture model with 32 mixtures
- Expectation-Maximization (EM) algorithm for training

$$p(x|\lambda) = \sum_{i=1}^{M} p_i b_i(x)$$

$$b_i(x) = \frac{1}{(2\pi)^{D/2}|\sum_i|^{1/2}} exp\{-\frac{1}{2}(x-\mu_i)^T(\sum_i)^{-1}(x-\mu_i)\}$$

Text-independent Speaker Identification Results

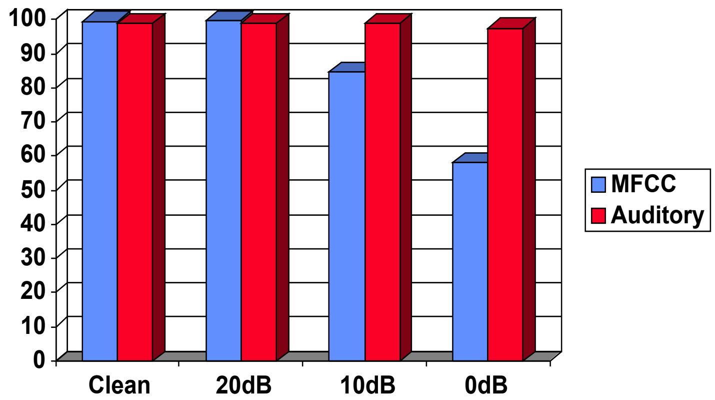

Car noise

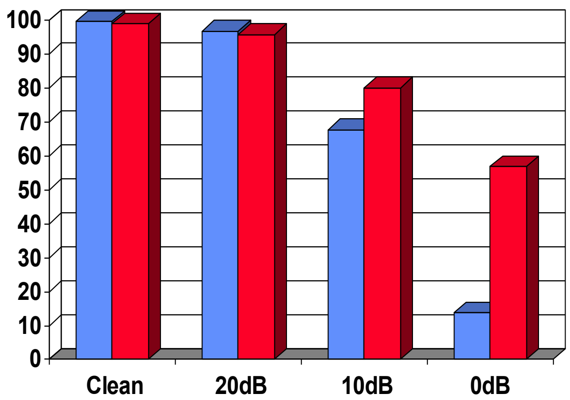

Babble noise

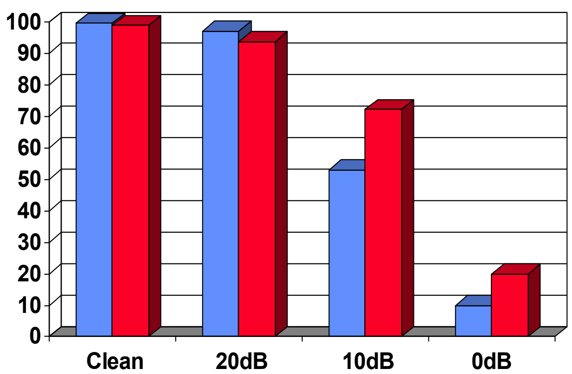

Factory noise

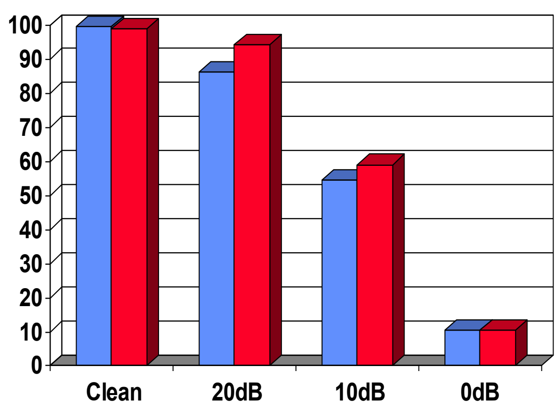

White noise

Event-Driven Sensory Adaptive Analog Processing

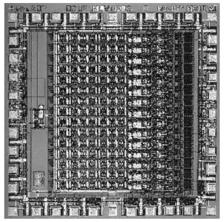

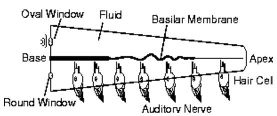

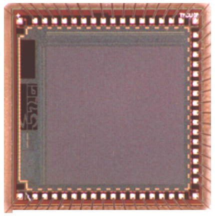

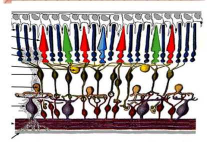

Mic, Ultrasonic transducer, Strain gauge, …

Time-frequency sensory event stream encoder

e.g. filterbank zero-crossings

AER time events

Imager, Touch screen, …

Spatiotemporal sensory event stream encoder

e.g. spatial gradient and temporal change amplitude threshold detections

AER time events

TDMA Asynchronous Bus

AER time events

Event stream transceiver and decoder

Sensor fusion, feature binding, and adaptive pattern recognition

Classification events

e.g. detection of glass break acoustic events

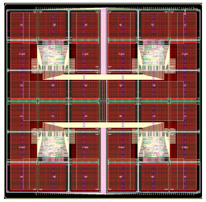

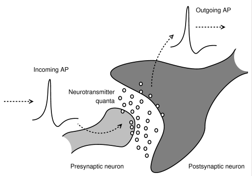

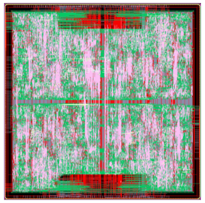

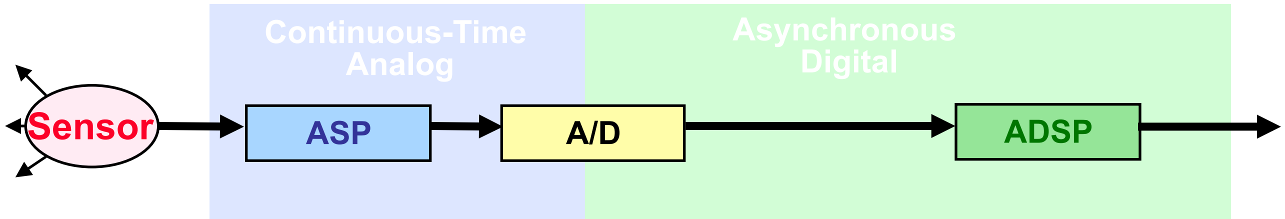

- Data driven
- Asynchronous
- Highly energy efficient
- Robust to additive noise in the signal

- Asynchronous routing of sensory address events
- Expandable integration of sensory modalities
- Reconfigurable and adaptive general-purpose signal processing and identification

Acoustic Source Separation and Localization

Bioinspired Smart Sensing Adaptive Microsystems

Tympanal directional hearing (*parasitoid fly*)

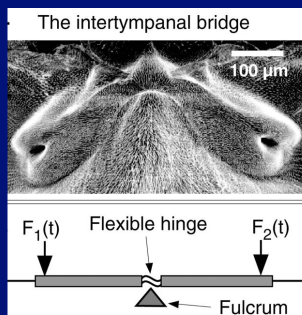

Biomorphic and Neuromorphic Engineering

Adaptation

Micropower, low-aperture acoustic source localization (*ISCAS'2004*)

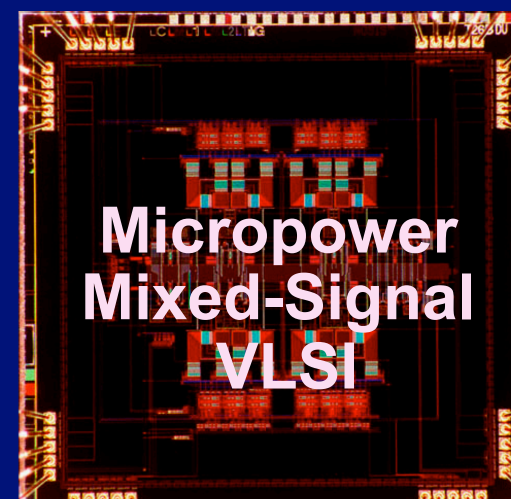

Biomechanics of Tympanal Directional Hearing

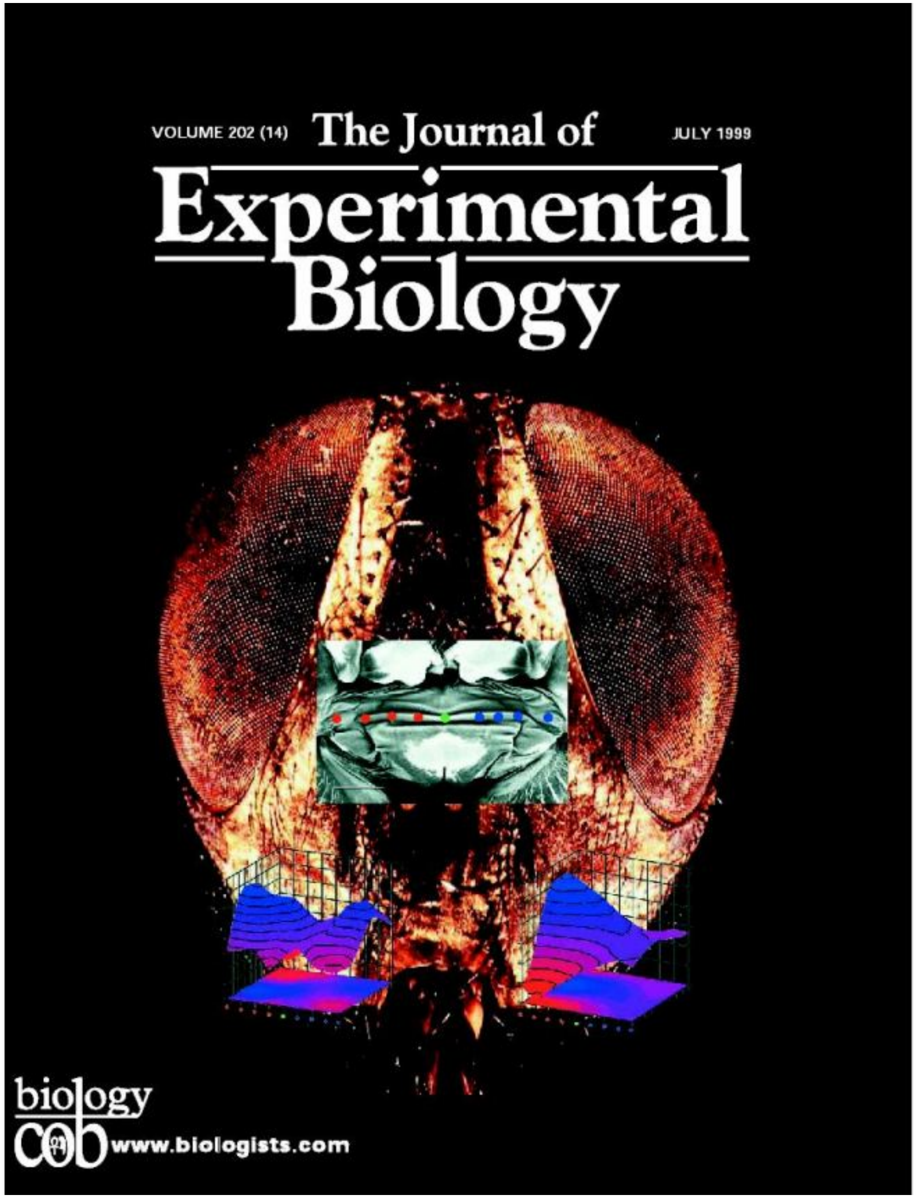

- Parasitoid fly localizes singing cricket by a beamforming acoustic sensor of dimensions a factor 100 smaller than the wavelength.
- Tympanal beamforming organ senses acoustic pressure gradient, rather than time delays, in the incoming wave.

Robert, D., Miles, R.N. and Hoy, R.R., 1999. "Tympanal hearing in the sarcophagid parasitoid fly Emblemasoma sp.: the biomechanics of directional hearing," *J. Experimental Biology* **202**: 1865-1876.

Auditory Anatomy and Temporal Acoustic Cues

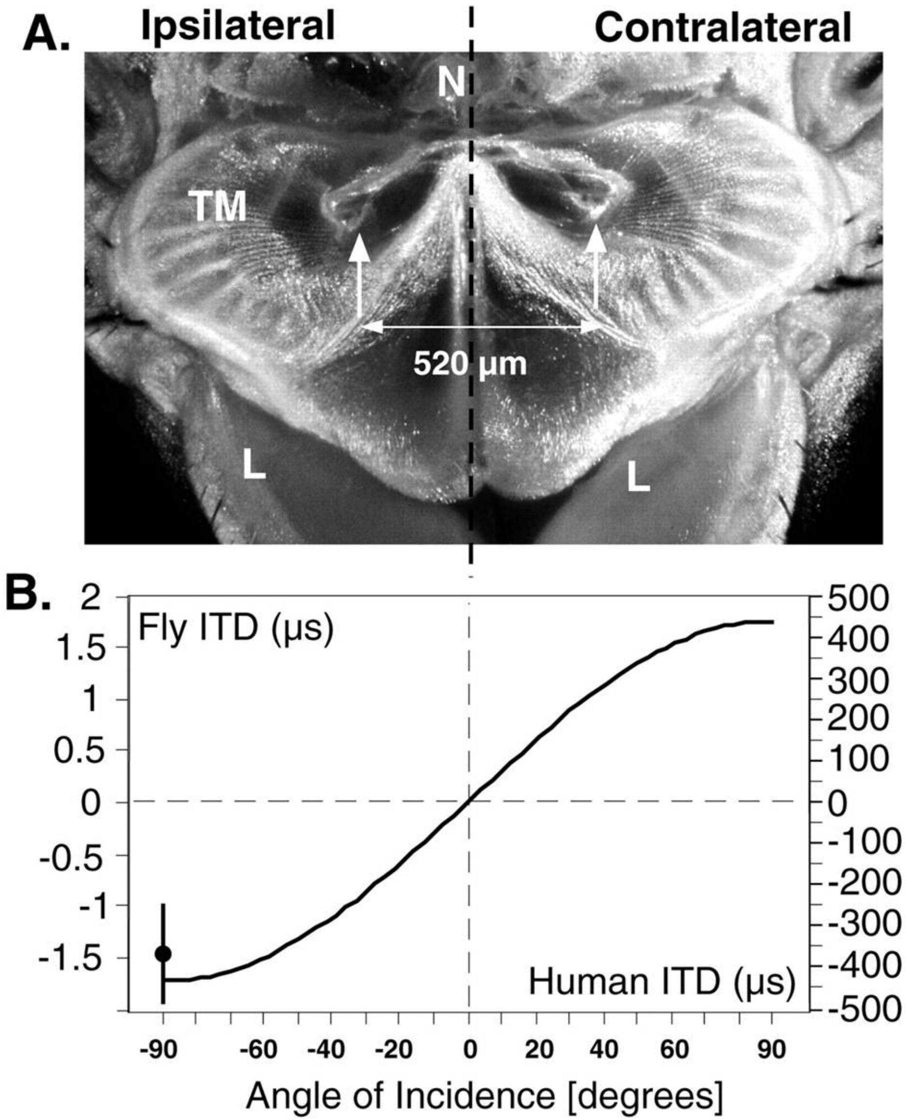

(A) The auditory organs of the parasitoid fly *Ormia ochracea* are located on the anterior thorax, between the first pair of legs (L) and the neck (N). The tympanal membranes (TM) are adjacent to each other and set close together by the midline of the animal (vertical dashed line). Providing a connection between the two TMs across the midline, the intertympanal bridge is made of thicker cuticle than TMs and has the shape of a coat hanger. Two depressions at both ends of the intertympanal bridge indicate the insertion point of the sensory organs (arrows). Arrows also point to the interaural distance.

(B) Interaural time difference (ITD) as a function of the angle of incidence of the sound stimulus. Right ordinate: ITDs calculated for humans (ear separation of 170 mm). Left ordinate: ITDs at the fly' s ears calculated for an interaural distance of 0.6 mm. Data point (with standard deviation) shows ITD measurement made at -90° azimuth and 5 kHz tone, with two probe microphones located at the TMs.

Robert, D., J. Amoroso, and R. R. Hoy. 1992. The evolutionary convergence of hearing in a parasitoid fly and its cricket host. *Science* **258**:1135–1137.

Mechanical Coupling Across the Intertympanal Bridge

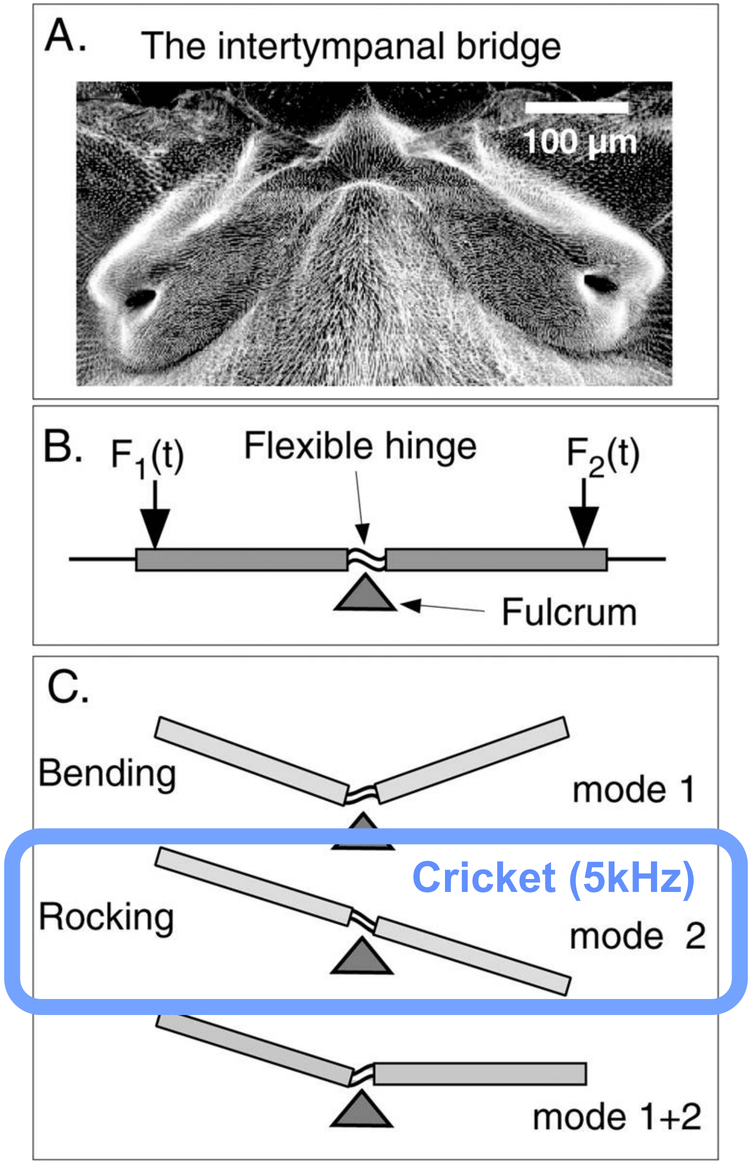

(A) Close-up of the intertympanal bridge connecting the tympanal membranes.

(B) Simple mechanical model of the bridge as a seesaw endowed with two rigid bars connected by a flexible central hinge (~).

(C) On the basis of the laser vibrometric micromechanical analysis, it is suggested that two basic modes can characterize the observed mechanical response. Bending occurred at low frequencies (mode 1; <4 kHz), whereas rocking was measured at intermediate frequencies (mode 2; 5–7 kHz). At higher frequencies (15 kHz and above), bending and rocking modes combine to elicit motion in one tympanum only (mode 1 + 2).

Robert, D., R. N. Miles, and R. R. Hoy. 1996. Directional hearing by mechanical coupling in the parasitoid fly *Ormia ochracea*. *J. Comp. Physiol. A* **179**:29–44.

Traveling Wave Gradients

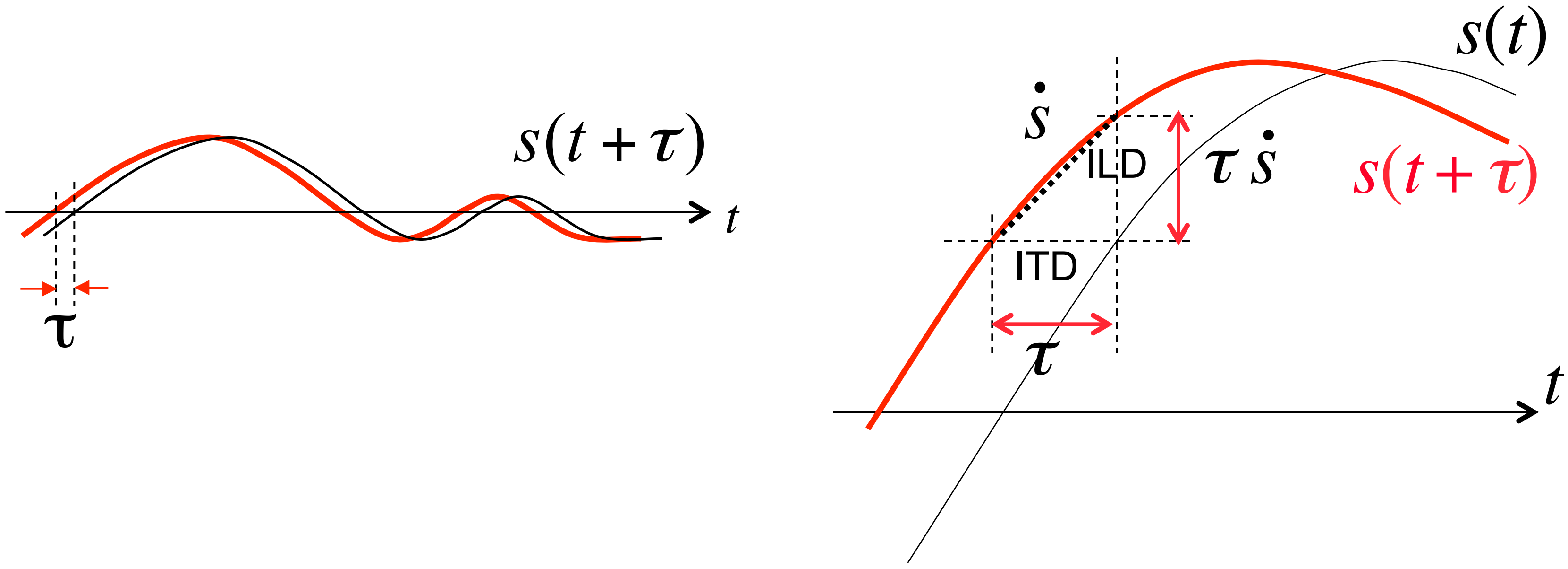

- For closely spaced acoustic sensors ("ears") as in the *Ormia*, interaural time delays (ITDs) are too short to be resolved with neural circuits.
- For sensor spacing closer than a wavelength (coherence interval), measurement of interaural level differences (ILDs) yields estimates of the ITDs, scaled by the time derivative of the acoustic signal.

Gradient Flow Localization

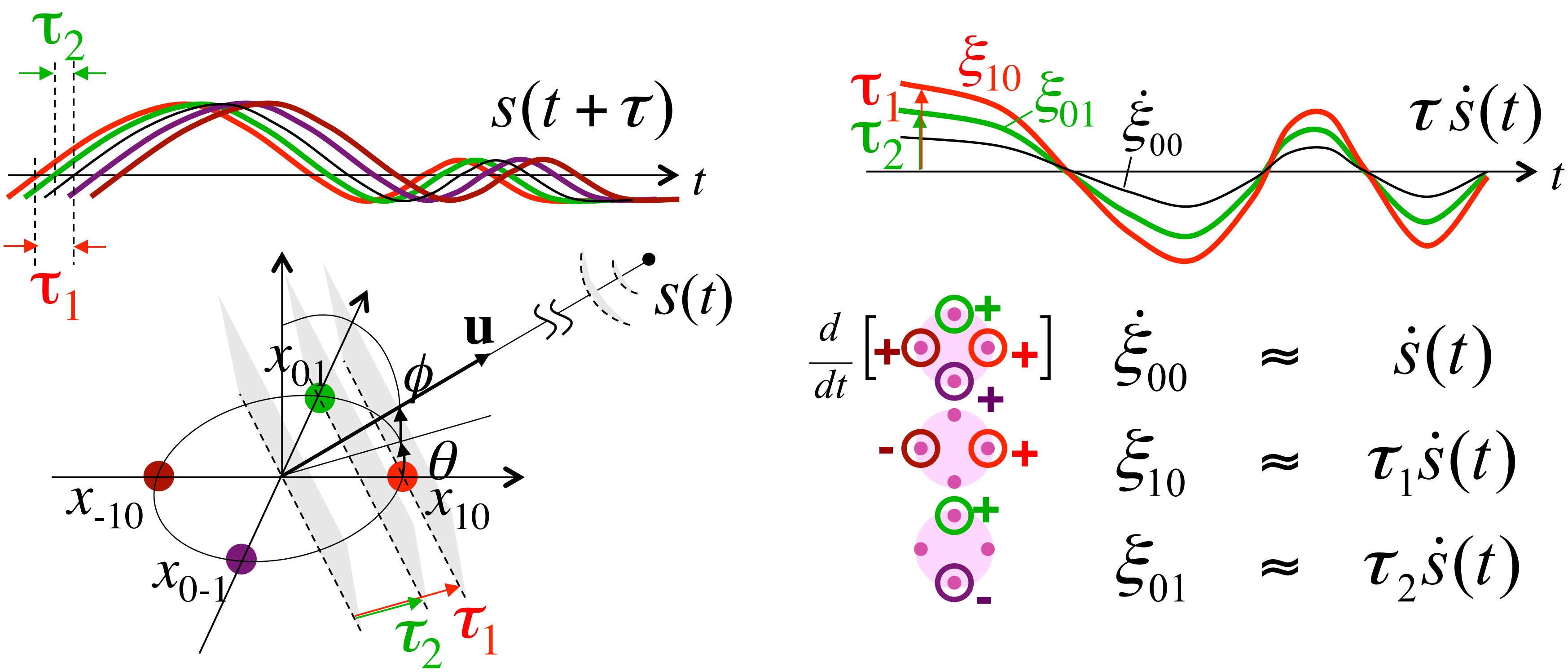

- *Gradient flow* obtains time delays at sub-sampling resolution by relating spatial and temporal differentials of the field across the array.
- 3-D direction cosines are obtained from a planar geometry with four sensors.

Gradient Flow Localization and Separation

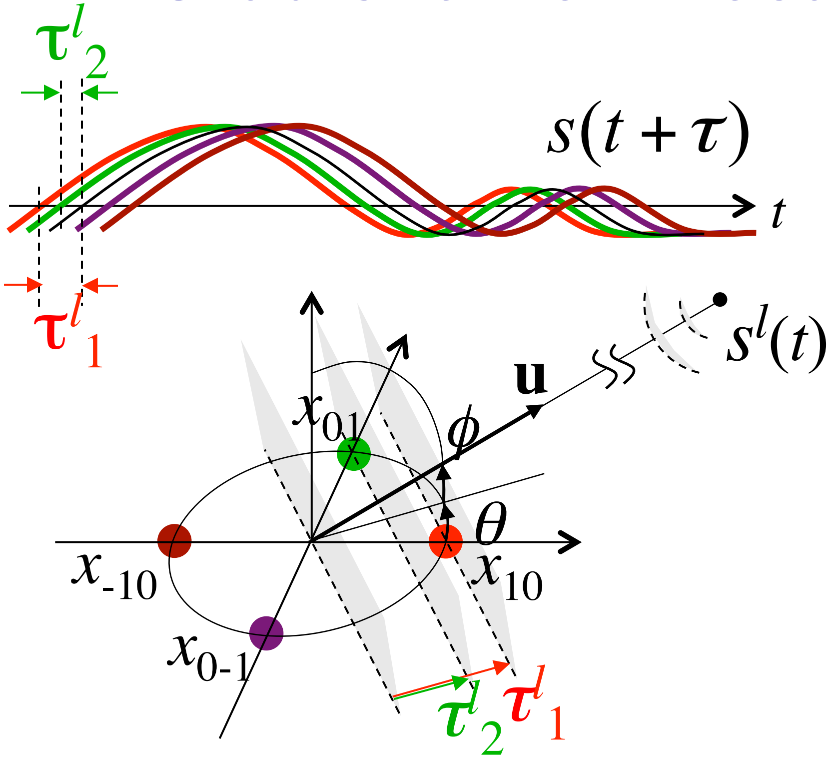

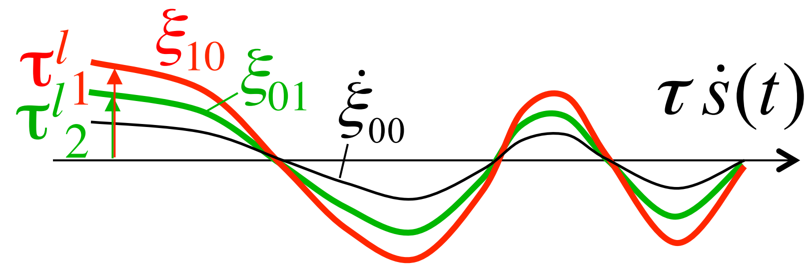

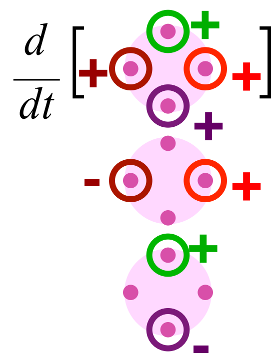

$$\dot{\xi}_{00} \approx \sum_\ell \dot{s}^\ell(t)$$

$$\xi_{10} \approx \sum_\ell \tau_1^\ell \dot{s}^\ell(t)$$

$$\xi_{01} \approx \sum_\ell \tau_2^\ell \dot{s}^\ell(t)$$

- Gradient signals from multiple sources add linearly. Sources are separated *and* localized with *independent component analysis* (ICA).

Barrere and Chabriel, IEEE TCAS-I, 2002
Cauwenberghs, Stanacevic and Zweig, ISCAS'2001

Differential Sensitivity

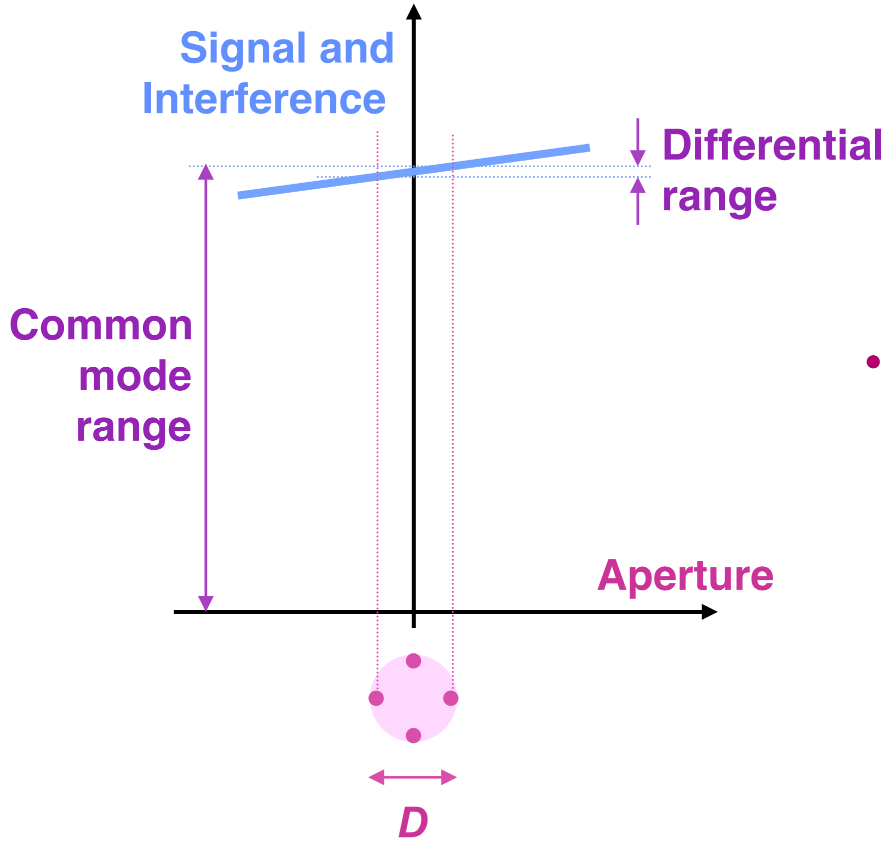

- **Gradient flow bearing resolution is fundamentally independent of aperture**
  - Cramer-Rao bound
  - Assumes interference noise dominates sensor/acquisition noise
- **In practice, aperture is limited by differential sensitivity in gradient acquisition**
  - Enhanced through differential coupling
    - *Mechanical*
      - ***Intertympanal bridge*** *[Robert, Miles and Hoy, 1996]*
    - *Electrical*
      - ***Latency/population encoding in auditory afferents*** *[Oshinsky and Hoy, 2002]*

Auditory Afferents in the *Ormia ochracea*

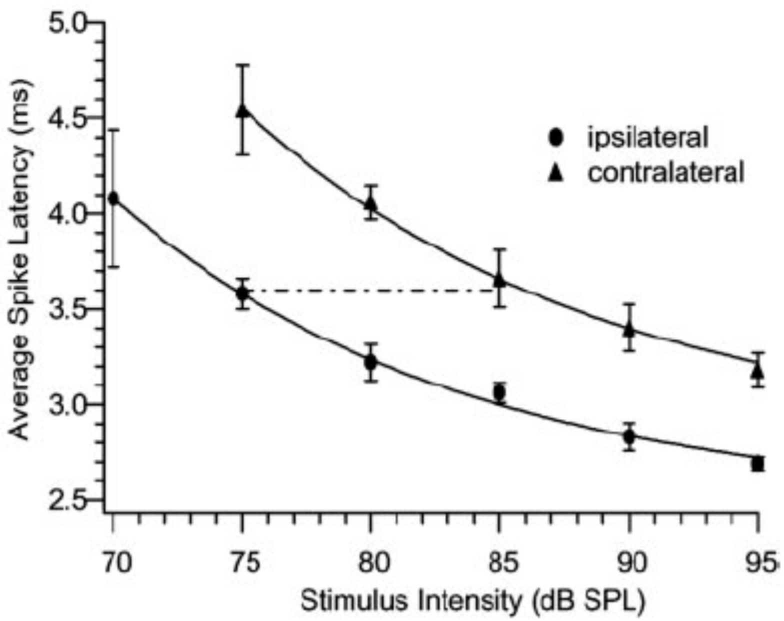

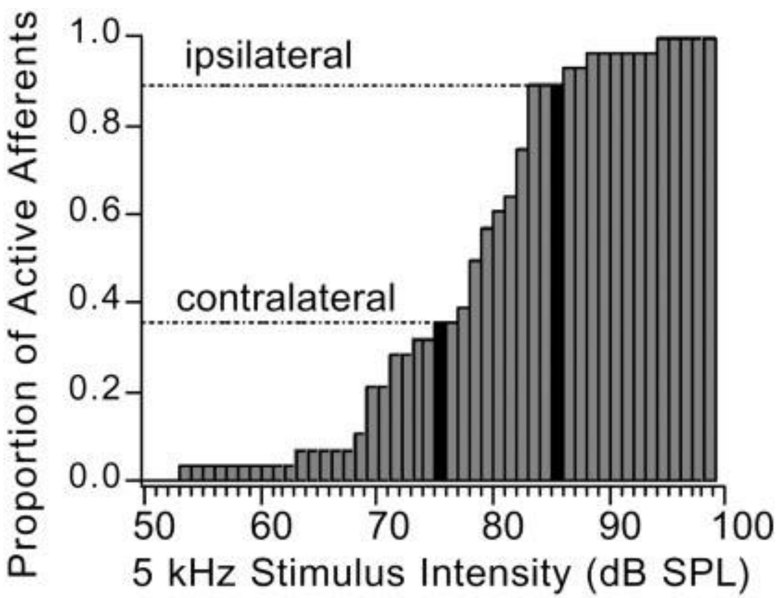

- **Latency Encoding**
- **Population Encoding**

Oshinsky ML, Hoy RR (2002), "Physiology of the Auditory Afferents in an Acoustic Parasitoid Fly," *J. Neurosci.* 22(16): 7254-7263.

Gradient Flow Super-Resolution Delay Estimation

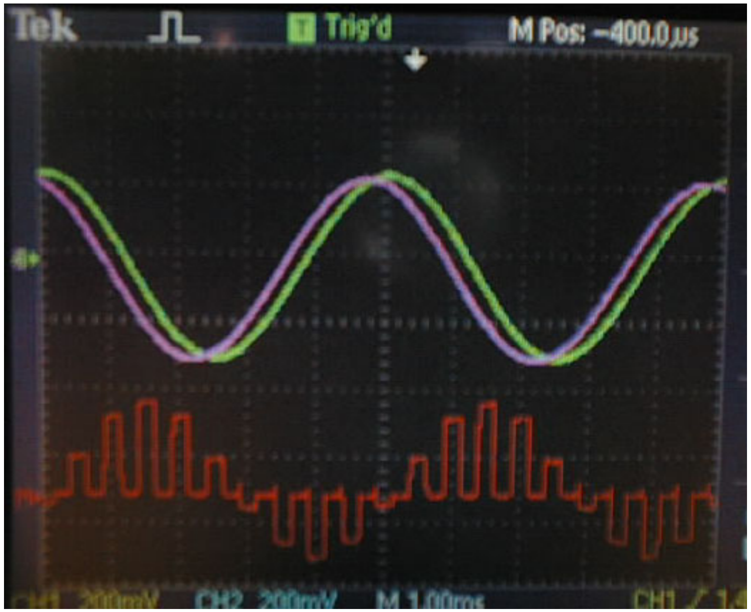

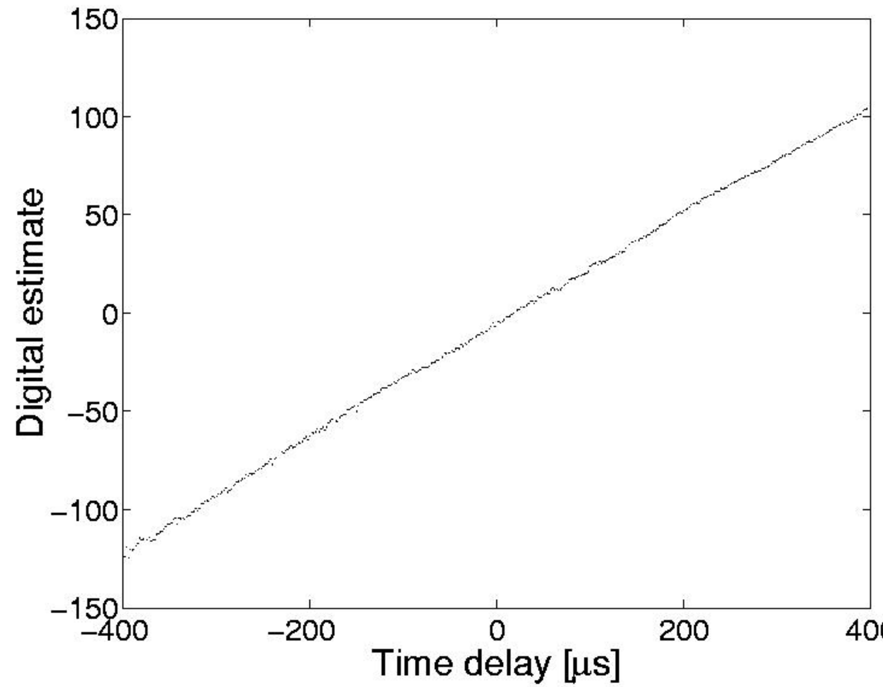

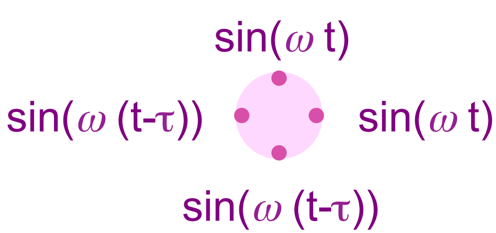

- **200 Hz signal**
- **2 kHz sampling frequency**
- **2μs delay resolution**

GradFlow/ASU Localization Experiments

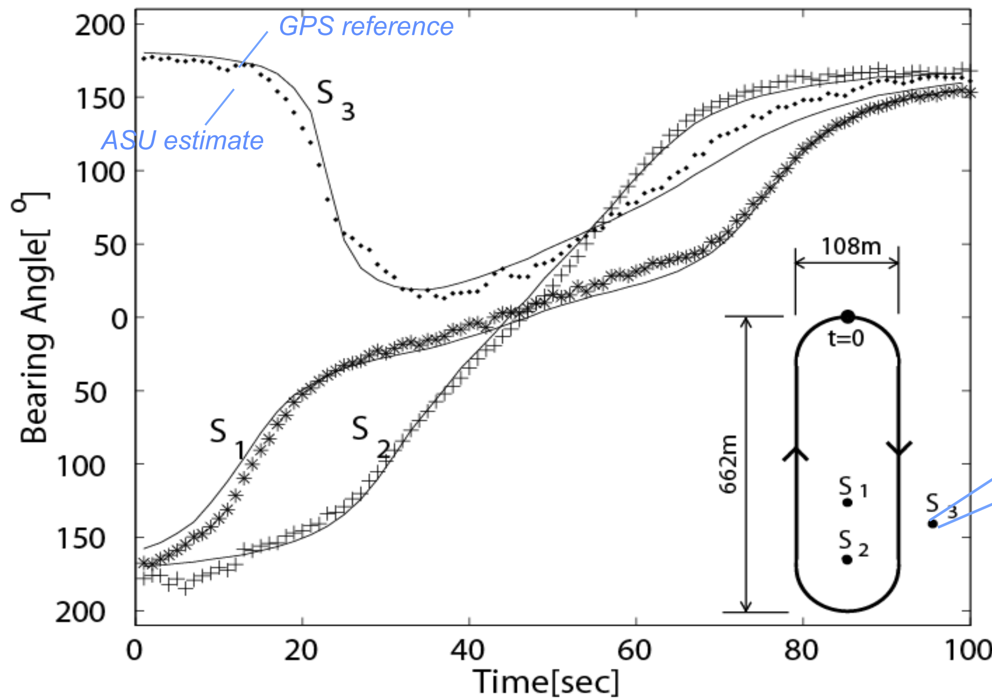

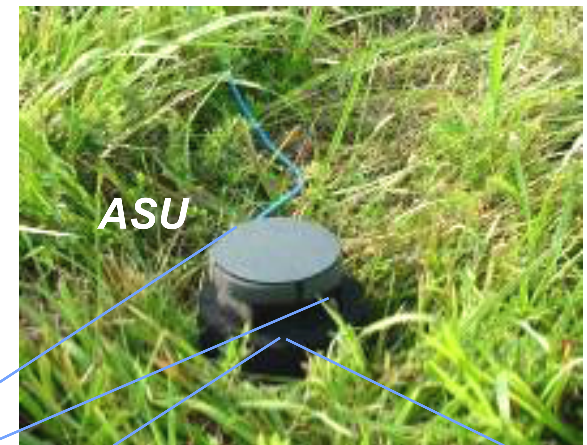

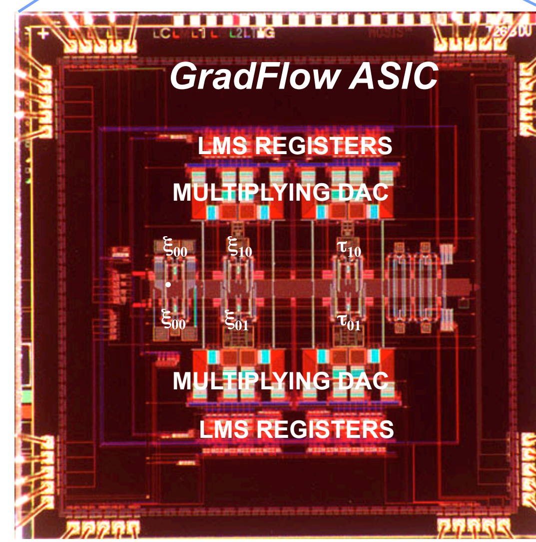

- **Acoustic Surveillance Unit (ASU)**
  Riddle et al., 2004
- **Integrated *GradFlow* ASIC**
  Stanacevic and Cauwenberghs, ESSCIRC' 2003
- **DARPA Aberdeen Proving Grounds field test:**
  – Sensor network with 3 ASUs
  – 5 degree bearing accuracy in tracking ground vehicles over 600m range
  – Tracked azimuth & elevation of overflying aircraft

•200 nsec resolution
• 16 kHz sampling
•54 μW power
• 3mm x 3mm in 0.5μm 3M2P CMOS

Gradient Flow Source Separation and Localization

Gradient flow on a mixture of acoustic waves reduces to a static (noisy) mixture problem:

$\frac{d}{dt}\left[\;\right]$ 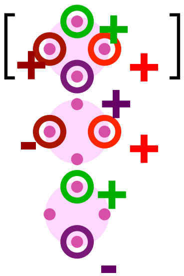

$$\begin{bmatrix} \dot{\xi}_{00} \\ \xi_{10} \\ \xi_{01} \end{bmatrix} = \begin{bmatrix} 1 & \cdots & 1 \\ \tau_1^1 & \cdots & \tau_1^L \\ \tau_2^1 & \cdots & \tau_2^L \end{bmatrix} \begin{bmatrix} \dot{s}^1(t) \\ \vdots \\ \dot{s}^L(t) \end{bmatrix} + \begin{bmatrix} \dot{\nu}_{00} \\ \nu_{10} \\ \nu_{01} \end{bmatrix}$$

$$\downarrow \qquad \downarrow \qquad \downarrow \qquad \downarrow$$

$$\mathbf{x} = \mathbf{A} \qquad \mathbf{s} + \mathbf{n}$$

observations	*direction vectors*	*sources*	*noise*
(gradients)		*(time-differentiated)*	*(gradients)*

solved by linear *static* ICA (Independent Component Analysis)

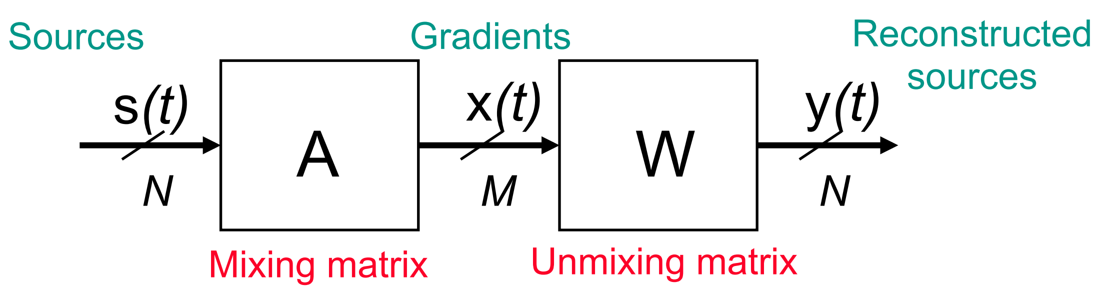

Gradient Flow Independent Component Analysis

integrated acoustic source separation and localization

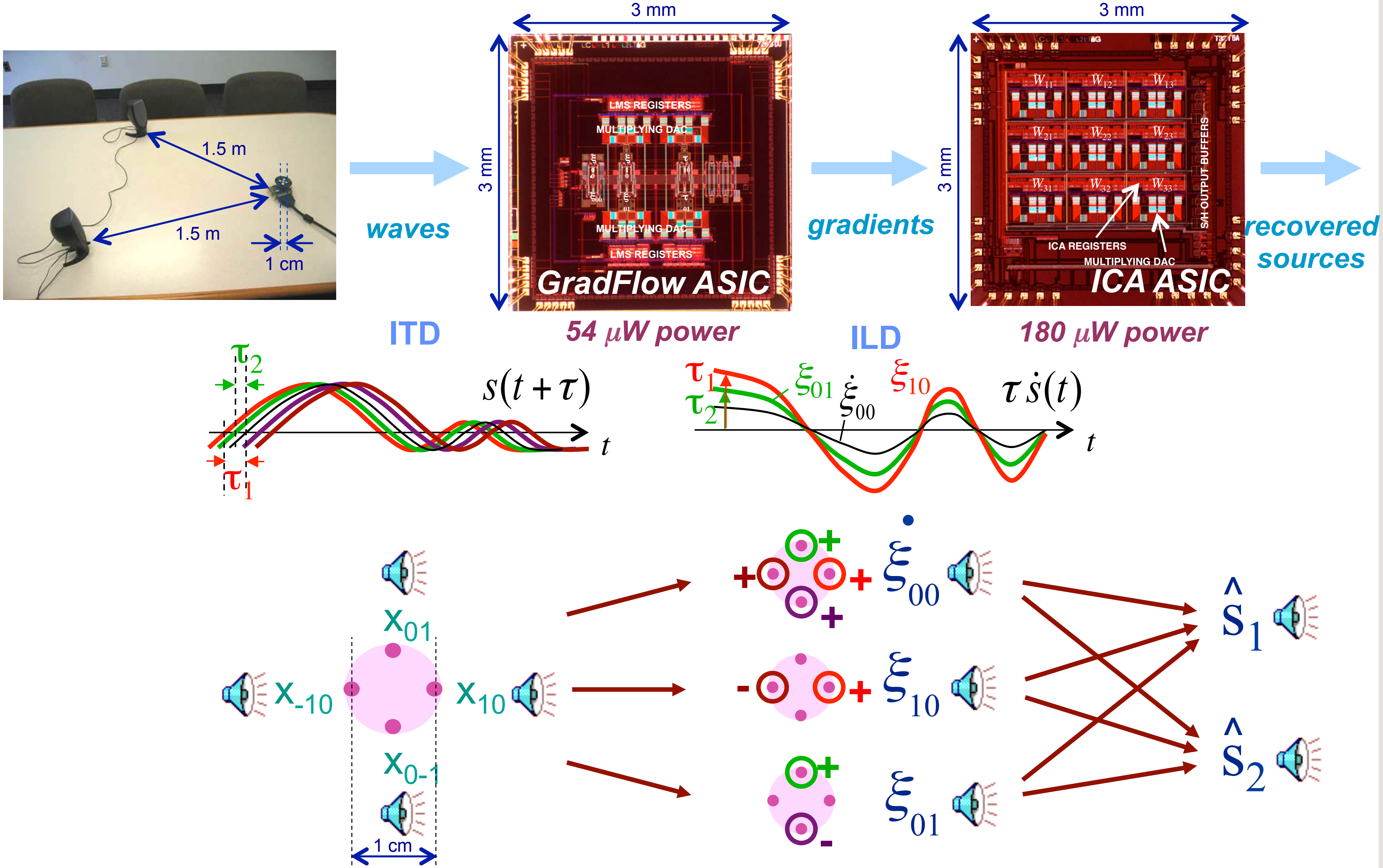

Gradient Flow ICA Residuals

crosstalk

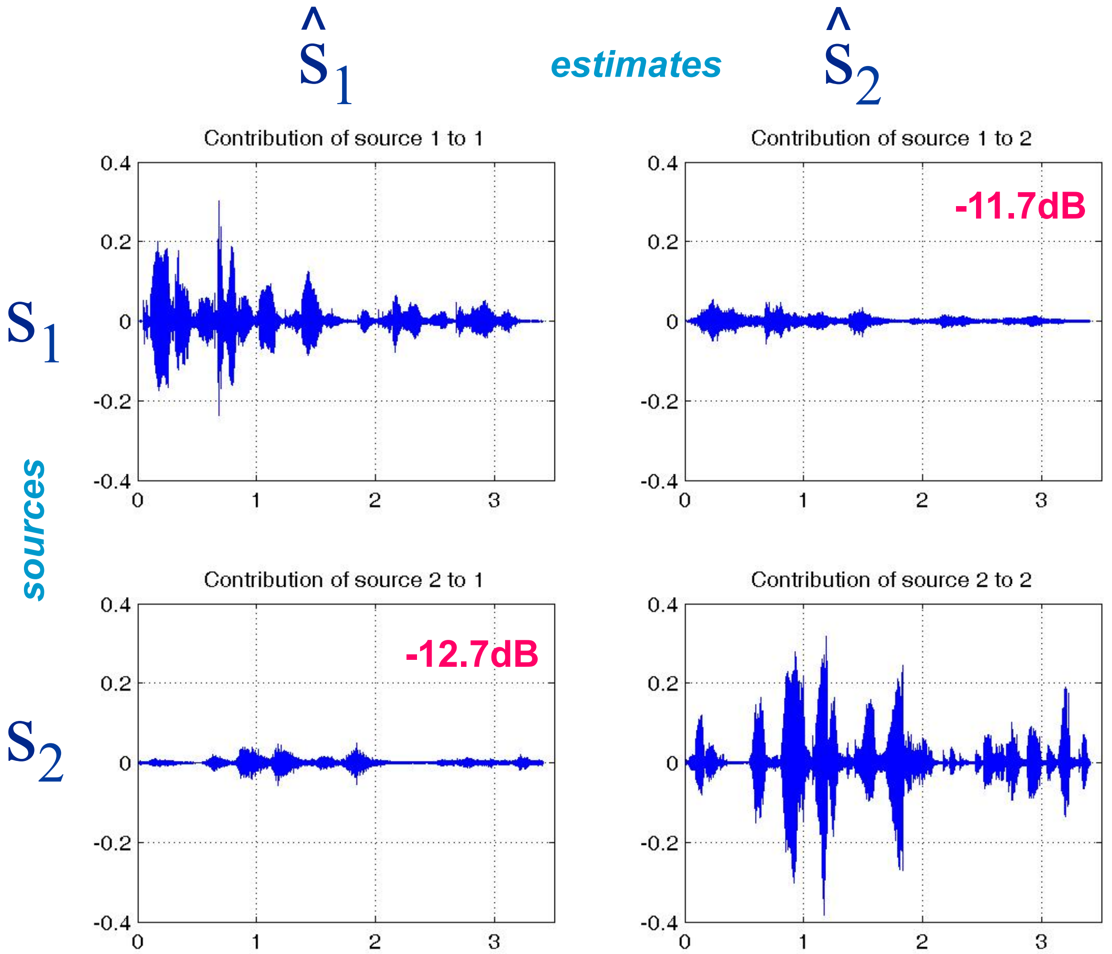

Gradient Flow ICA Residuals

crosstalk and reverberation

$\hat{s}_1$ *estimates* $\hat{s}_2$

sources

s_1

s_2

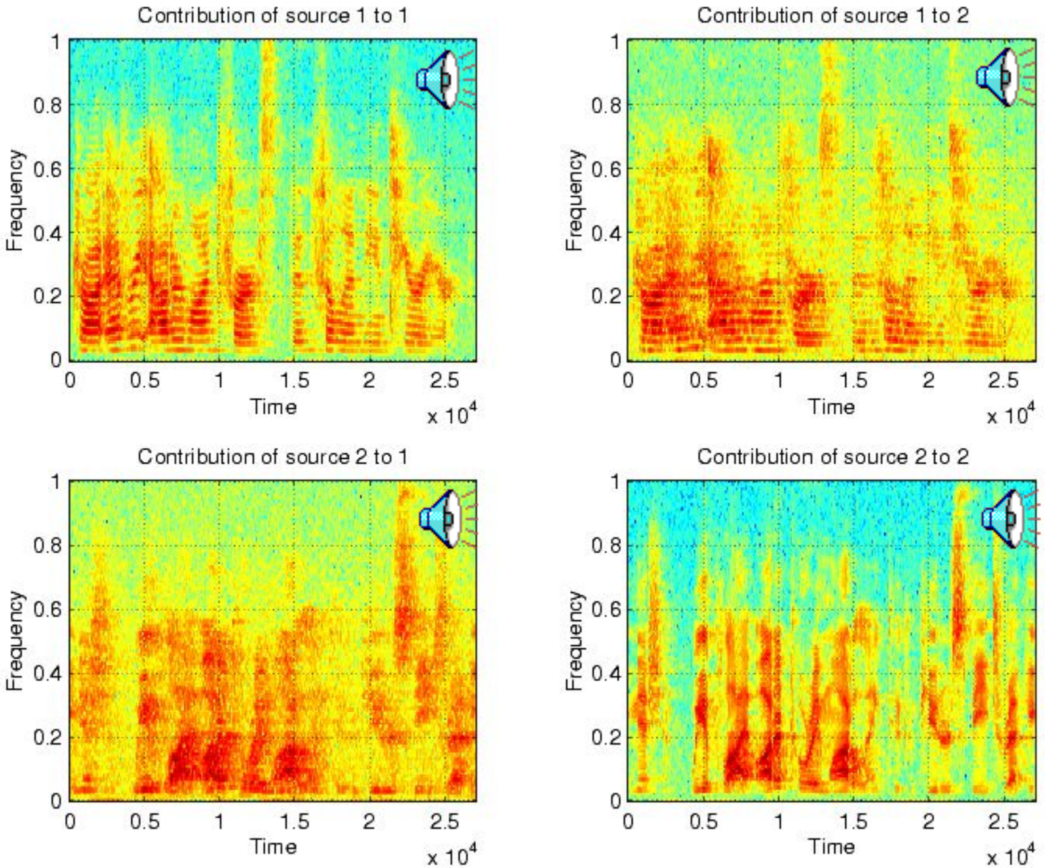

Crosstalk is virtually free of the direct path

- *Reverberation can be eliminated using LMS adaptive filtering of the ICA outputs*
- *Direction cosines of recovered sources correspond to the direct path*

Hearing Aid Implications

- Gradient flow localizes sources in three dimensions, and produces a linear instantaneous mixture of the sources that is conveniently separated using independent component analysis (ICA).
- ICA leads to adaptive suppression of several sources of noise and unwanted signals, independent of their angle of arrival.
- Gradient flow combined with ICA offers more flexibility in the choice of signal to be amplified and presented to the listener. The signal can be chosen based on the direction of arrival with respect to microphone array, or based on the power of the signal.

Directional Selectivity in Hearing Aids

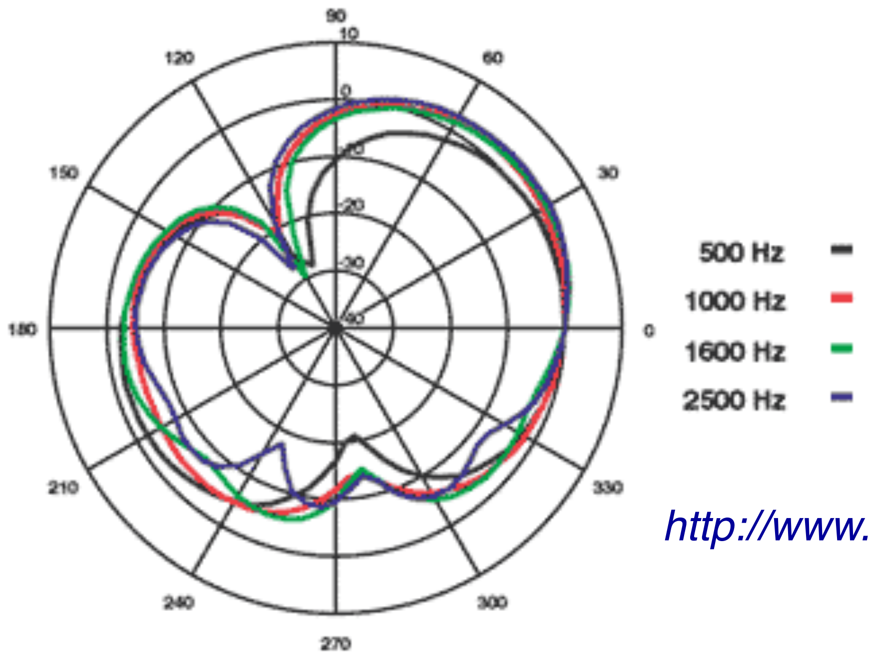

http://www.oticon.com

- **'State of the Art'**
  - Two microphones allow for one null angle in directionality pattern
  - Adaptive beamforming allows to steer the null to noise source
  - Presence of multiple noise sources requires source localization and separation with multiple microphones

Gradient Flow ICA Microphone

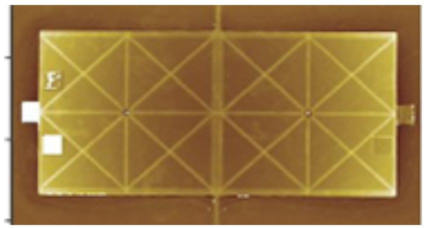

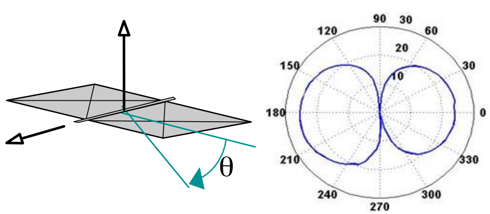

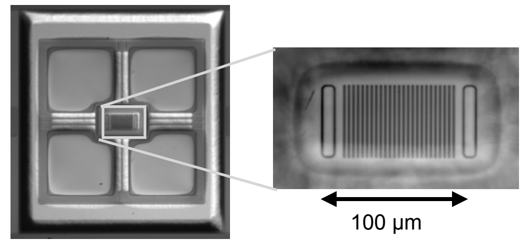

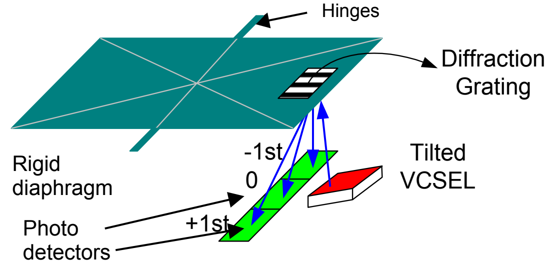

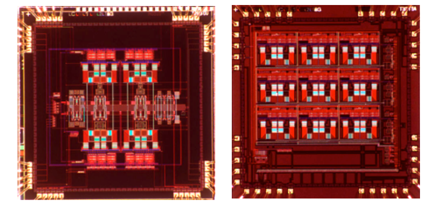

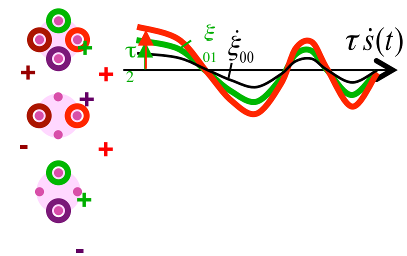

Differential Mechanical Sensing

Ron Miles, SUNY Binghamton

- MEMS microphone
- Models Ormia's inter-tympanal bridge mechanical coupling

Differential Optical Transduction

Levent Degertekin, Georgia Tech

- Optical microphone
- Diffractive optical sensing of membrane displacement
- Improved sensitivity and noise (<20dB spl)

Differential Electronic Signal Processing

- Gradient flow amplification
- ICA separation and localization
- Micropower chips (<250 uW)

Opportunities for In-Ear Health Sensing

- **Prevalence of wireless personal audio devices:**



- **Rapidly aging global population:**
  - Over the next few decades, people 65 years and older will account for **20% of the global population**, an unprecedented shift. New healthcare challenges and opportunities will arise for which **reliable and continuous high-bandwidth health data will be critical**.

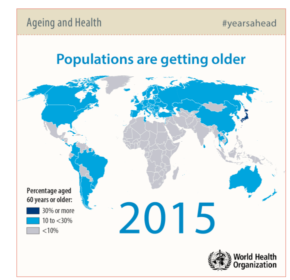

- **In-Ear Health Sensing Platform**
  - An in-ear healthcare platform has the convenience, comfort, and discretion of a consumer audio device, while offering valuable electrophysiological and bio-chemical data.

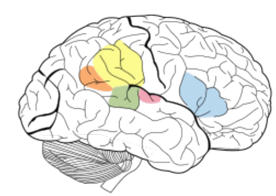

In-Ear Electrophysiology

Paul et al, IEEE NER 2019; IEEE EMBC 2019

High-density dry-contact electrodes capture a wealth of physiological information from an integrated in-ear device

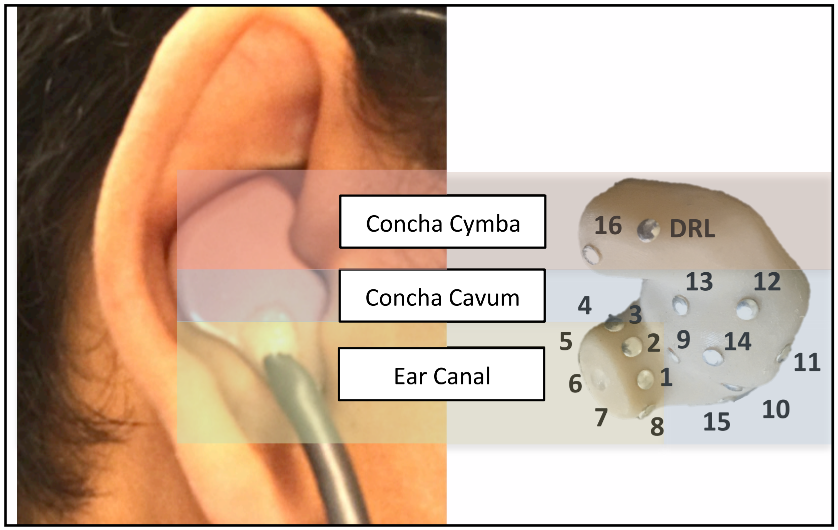

Auditory ERP

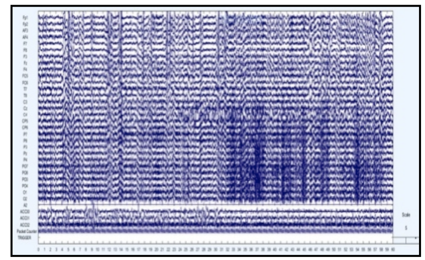

Electrodermal Activity

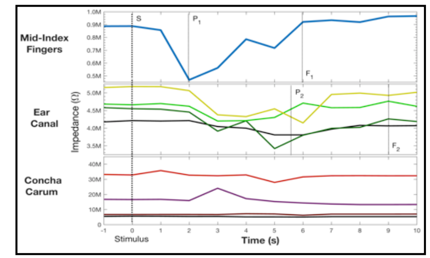

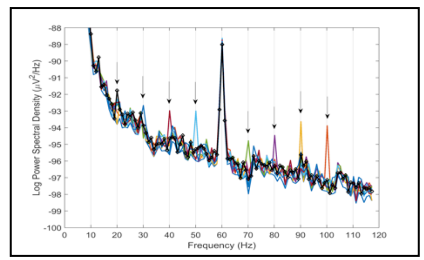

ASSR PSD

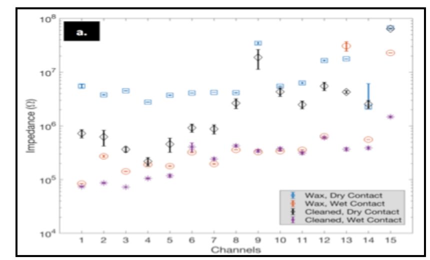

Impedance Imaging

- In-ear, high-density dry-contact electrode recording platform records electroencephalography (EEG) signals from the brainstem, temporal, and visual cortexes with quality comparable to commercial scalp EEG.
- Electrical impedance measurement provides electrodermal activity (EDA).
- Opportunities for closed-loop auditory neurofeedback (tinnitus, insomnia, apnea, etc).

Paul, A., Deiss, S., Tourtelotte, D., Kleffner, M., Zhang, T., and Cauwenberghs, G. Electrode-Skin Impedance Characterization of In-Ear Electrophysiology Accounting for Cerumen and Electrodermal Response. IEEE EMBS Int. Conf. Neural Engineering (NER'19), 2019.

Paul, A., Akinin, A., Cauwenberghs, G. Integrated In-Ear Device for Auditory Health Assessment. 2019 41st Annual International Conference of the IEEE Engineering in Medicine & Biology Society (EMBC'19), 2019.

Event-Driven Sensory Adaptive Analog Processing

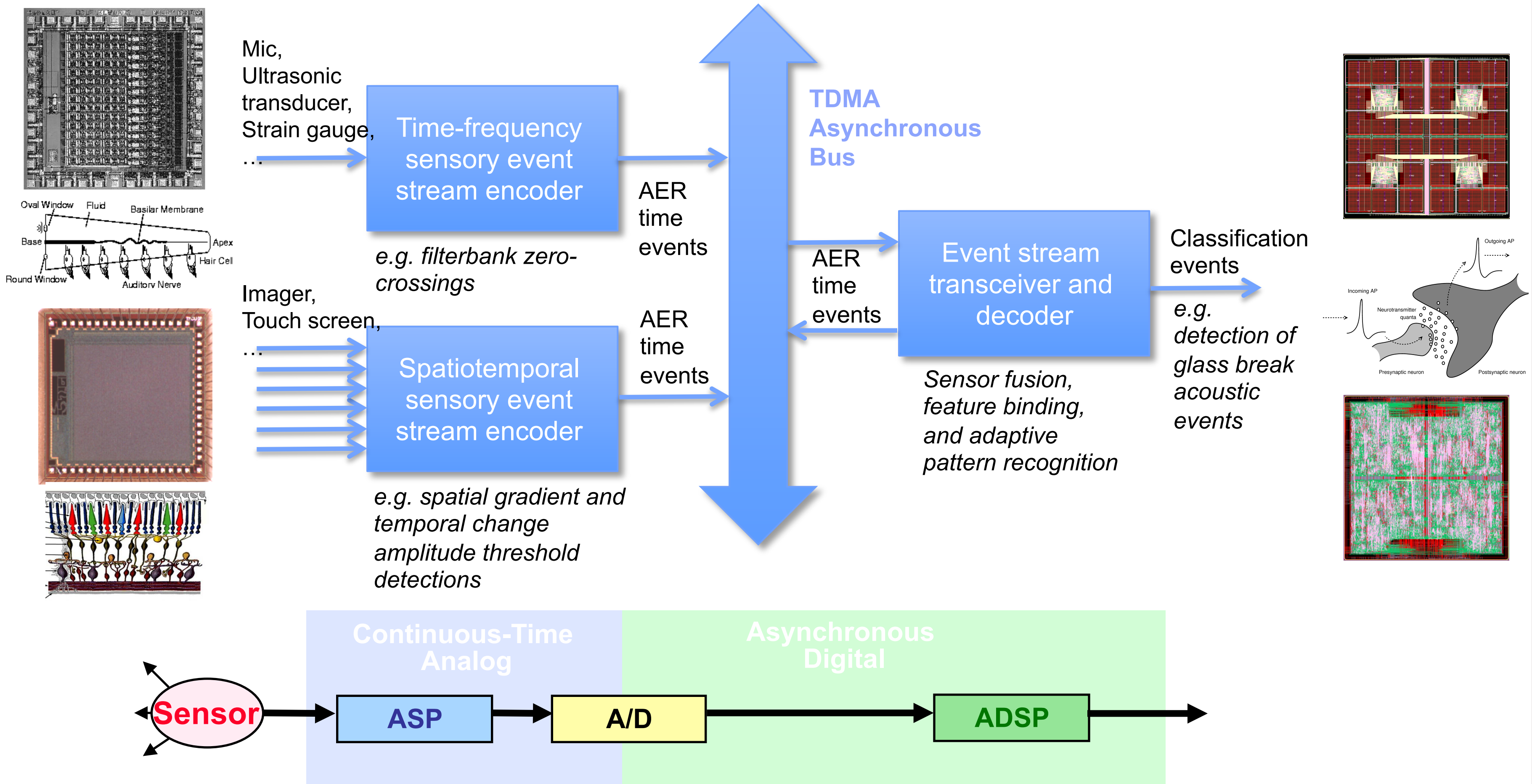

- Data driven
- Asynchronous
- Highly energy efficient
- Robust to additive noise in the signal

- Asynchronous routing of sensory address events
- Expandable integration of sensory modalities
- Reconfigurable and adaptive general-purpose signal processing and identification

BENG 207 Neuromorphic Integrated Bioelectronics

Date	Topic
9/27, 9/29	Biophysical foundations of natural intelligence in neural systems. Subthreshold MOS silicon models of membrane excitability. Silicon neurons. Hodgkin-Huxley and integrate-and-fire models of spiking neuronal dynamics. Action potentials as address events.
10/4, 10/6	Silicon retina. Low-noise, high-dynamic range photoreceptors. Focal-plane array signal processing. Spatial and temporal contrast sensitivity and adaptation. Dynamic vision sensors.
10/11, 10/13	Silicon cochlea. Low-noise acoustic sensing and automatic gain control. Continuous wavelet filter banks. Interaural time difference and level difference auditory localization. Blind source separation and independent component analysis.
10/18, 10/20	Silicon cortex. Neural and synaptic compute-in-memory arrays. Address-event decoders and arbiters, and integrate-and-fire array transceivers. Hierarchical address-event routing for locally dense, globally sparse long-range connectivity across vast spatial scales.
10/28, 11/1	Review. Modular and scalable design for neuromorphic and bioelectronic integrated circuits and systems. Design for full testability and controllability.
11/1, 11/3	Midterm due 11/2. Low-noise, low-power design. Fundamental limits of noise-energy efficiency, and metrics of performance. Biopotential and electrochemical recording and stimulation, lab-on-a-chip electrophysiology, and neural interface systems-on-chip.
11/8, 11/10	Learning and adaptation to compensate for external and internal variability over extended time scales. Background blind calibration of device mismatch. Correlated double sampling and chopping for offset drift and low-frequency noise cancellation.
11/15, 11/17	Energy conservation. Resonant inductive power delivery and data telemetry. Ultra-high efficiency neuromorphic computing. Resonant adiabatic energy-recovery charge-conserving synapse arrays.
11/22, 11/24	Guest lectures
11/29, 12/1	Project final presentations. All are welcome!